PHILCO

A SUBSIDIARY OF Ford Motor Company

RESEARCH LABORATORIES

PHILCO
A SUBSIDIARY OF Ford Motor Company
RESEARCH LABORATORIES

Publication No. U-2771
W. O. 2016

FINAL TECHNICAL REPORT

LASER PUMPING SOURCES

Prepared for: Advanced Research Projects Agency
Washington, D. C.

Under Contract: NOnr 4237(00)
ARPA Order No. 306-62
Project Code No: 3730
Date of Contract: 16 June 1963
Contract Expiration Date: 15 June 1964
Project Scientist: S. Byron
ORiole 5-1234
Newport Beach, California

Prepared by: S. Byron, J. Killian, H. Shanfield, D. Peters, W. Lawrence

Approved by: Paul H. Lotter, Jr.
M. H. Johnson, Director
Physics Laboratory

This research is a part of Project DEFENDER, under joint sponsorship of the Advanced Research Projects Agency, the Office of Naval Research, and the Department of Defense.

15 July 1964

CONTENTS

ILLUSTRATIONS

ILLUSTRATIONS (CONTINUED)

LIST OF TABLES

SECTION 1

SUMMARY

The direct conversion of stored chemical energy to radiation suitable for pumping laser materials was investigated under this contract. Both explosives and pyrotechnics were studied as well as the possibilities offered by combining the two. In this program the emphasis was on gaining an understanding of the fundamental limitations in producing high radiation intensity, long pulse duration, and high overall energy conversion efficiency for these radiation sources.

The principles and practice of the conversion of explosive energy to shock heated gas energy suitable as a radiation source were reviewed. From this it was concluded that there are three major limiting factors associated with adapting explosive light sources developed previously to laser pumping: (1) these sources are destructive in nature, resulting in loss of costly laser crystals, (2) the overall energy conversion efficiency achieved previously is very low, and (3) the radiation brightness temperature is limited to about 20,000°K.

To overcome the first two of these fundamental limitations a major modification of the early argon flash bomb was conceived and studied experimentally as part of this program. Two seemingly simple changes were incorporated, involving (1) the use of stationary reflected shock heated gas as the radiation source rather than the use

of high speed incident shock heated gas and (2) the use of sub-atmospheric xenon as the gas to be shock heated. This allows in principle, an order of magnitude increase in radiation pulse duration, and two orders of magnitude decrease in mass of explosive used. Although a number of difficulties were encountered in carrying this out, the final experiments demonstrated the remarkable improvement in performance made possible by these changes. A radiation pulse was produced over a stationary area of 5 cm^2 having a peak brightness temperature (at a wavelength of 5600 A) of 12,300°K, which remained above 6000°K for a duration of 450 microseconds. This was produced using only 1 gram of stored chemical energy. This radiation source was used subsequently to stimulate laser action in a neodymium doped glass rod, causing no damage to the laser crystal.

From the analysis and the experimental results it is concluded that the shocked gas chemical radiation source yields high energy conversion efficiencies at temperatures up to about 15,000°K. However, further increase in intensity can be accomplished only by sacrificing overall energy conversion efficiency.

The radiation characteristics of pyrotechnics and explosive-pyrotechnic combinations were studied in an attempt to produce elevated radiation temperatures, suitable for high intensity pumping of laser crystals. Initial measurements were made of the spectral emission from zirconium-oxygen pyrotechnics ignited by a small (50 joule) electrical discharge. Results showed that the emission at 5600 A corresponds to that of a blackbody at a temperature several hundred degrees Kelvin below the theoretically predicted flame temperature. The use of elevated pressures to increase the flame temperature was studied in an optical bomb, showing an increase in brightness temperature with increasing pressure, but limited to peak values of 4790°K at 1000 psi oxygen pressure. In an effort to generate even higher flame and radiation temperatures the combined use of explosives and pyrotechnics was studied, resulting in temperature

increases of a few hundred degrees Kelvin. Higher brightness temperatures were also sought by taking advantage of chemiluminescence of reactants injected together and heated by small explosive charges, but failed because of the intrusion of the explosive products.

These results, in accord with information gathered at other laboratories on other chemical systems, strongly indicates that there is a fundamental upper limit in the radiation intensity that can be achieved directly from high energy density chemically reacting systems. This intensity limit corresponds to an effective brightness temperature of about 5000°K in the visible range of the spectrum.

SECTION 2

SHOCKED GAS CHEMICAL RADIATION SOURCE FOR LASER PUMPING

2.1 BASIC PRINCIPLES

The experimental and analytical studies of this concept in chemical pumping were aimed at understanding the basic principles and discovering what fundamental limitations are associated with this approach. The parameters of prime concern were overall energy conversion efficiency and maximum pumping intensity.

The earlier development of the argon flash bomb[1] served as a starting point in the exploitation of the shocked gas chemical laser pump. This device was developed many years ago for use in backlighting experimental studies of high explosives. The radiation source, shown schematically in Figure 1, was generated in a tube about a foot long by a very strong shock compression of argon gas at one atmosphere initial pressure, driven by detonation of a shaped explosive charge weighing 1/4 to 1 pound. The argon is heated to temperatures well over 10,000°K, the value above which it is highly luminous by virtue of Bremsstrahlung emission from electrons colliding with each other and with the ions and atoms. Evaluation of the overall energy conversion efficiency of this radiation source as previously developed indicated disappointingly low values. Less than one tenth of one percent of the stored chemical energy was actually released as radiation. It became clear early in this study that the causes for this low efficiency must be discovered and overcome, if possible.

BLANK PAGE

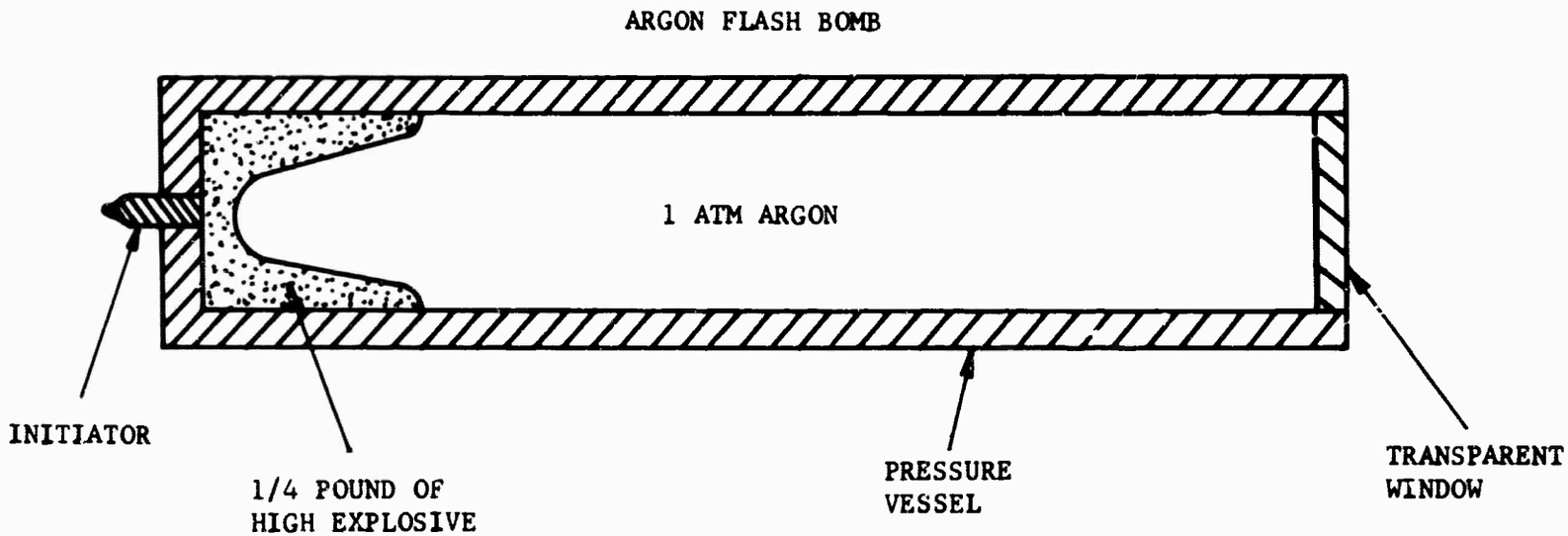

FIGURE 1. SCHEMATIC OF THE ARGON FLASH BOMB ILLUMINATOR DEVELOPED PREVIOUSLY FOR BACKLIGHTING STUDIES OF EXPLOSIONS.

In the early months of this program an analysis of the argon flash bomb led to a qualitative understanding of the origin of the low energy conversion efficiency. This analysis is based on the earlier experimental observation[1] that the radiation intensity corresponds to blackbody radiation at 15,000°K to 20,000°K, but the duration is only 50 μsec. Thus a maximum of 20 to 50 joules per square centimeter of radiating surface area could be released. Using a tube 5 cm in diameter, typical of the light sources actually used, a maximum of about 1000 joules of radiation energy is released from a device which contains about 10^6 joules of chemical energy stored in the 1/2 pound explosive charge. This overall energy conversion efficiency of 0.1% is a factor of about 100 smaller than could reasonably be expected.

There are only two steps in this energy conversion process; the chemical energy is first converted to shocked gas energy, and the shocked gas energy is then released in the form of radiation. Measurements of the shock wave speed indicated shock Mach numbers up to about 40 in argon which correspond to a thermal energy of about 20 joules per cubic centimeter of original gas volume. In a 5 cm diameter, 30 cm long tube the argon is capable of storing about 20,000 joules of thermal energy, only 2% of the chemical energy actually available. This clearly represents a major energy loss process.

However the conversion of the stored thermal energy of the shock heated gas to radiation energy is also quite inefficient. Based on the calculations above a maximum of 5% of the gas energy is liberated in radiation over all wavelengths. If emission from the shock heated gas toward the explosive products could be utilized, this could be increased to 10%. The basic reason for this 10% limitation is that the duration of the radiation is limited to about 50 μsec by the arrival of the shock at the end of the tube and subsequent destruction of the optical window and/or mixing with ambient air. If the shock heated gas remained intact it would have a natural radiation cooling time of about 500 μsec.

In considering the various possibilities for improving the efficiency of this energy conversion process, it is readily apparent that small modifications of the basic argon flash bomb could not yield the orders of magnitude improvement in performance that should be possible. For example, a simple reduction of the size of the explosive charge results in a slower shock and a corresponding reduction in the radiation intensity, providing little or no improvement in energy conversion efficiency. Substitution of xenon for argon would increase the efficiency of converting chemical energy to thermal energy stored in the gas, but without a corresponding increase in radiation pulse duration the overall energy conversion efficiency would be increased only slightly.

A major revision in the concept appeared necessary, one which would increase the radiation pulse duration by an order of magnitude and simultaneously decrease the amount of explosive used by two orders of magnitude. An approach designed to accomplish this was conceived and studied experimentally as part of this program. Final results obtained near the end of the contract verified that a high overall energy conversion efficiency was achieved; using only 1 gram of combustible material and 1.5 grams of xenon a radiation pulse having a peak brightness temperature of 12,000°K and lasting 450 μsec was produced. The intensity decayed roughly linearly with time from a brightness temperature of 10,000°K at 160 μsec to 6000°K at 450 μsec.

This increase in radiation pulse duration by one order of magnitude was accomplished by making use of both the incident and reflected shock waves to produce a stationary high temperature radiating gas. In addition, by utilizing xenon at subatmospheric initial pressures as the shock heated gas, it was possible to reduce the amount of combustible chemicals by two orders of magnitude from 1/2 pound to 1 gram. This modification was not without difficulties, however. A number of serious problems cropped up in the course of proving out this concept and are discussed below in detail.

2.2 EXPERIMENTAL EQUIPMENT

The linear shock tube shown in Figure 2 was used to investigate the fundamental principles and limitations associated with the shocked gas radiation source, modified as noted above. The driven section of the tube was evacuated and filled with xenon or argon at initial pressures ranging from 100 mm Hg to 1 atmosphere. This section of the shock tube was equipped with 3 solid state photodiodes to sense shock arrival time at each of 3 windows, providing two measurements of shock speed. At the end of the tube a short section was located containing two openings for viewing radiation from the incident shock heated gas as well as the reflected shock heated gas. Light emitted through the first optical aperture (1/16" opening) which may or may not be covered by a window was transmitted through a 1/8" aperture and focused on the entrance slit of a spectroscope or monochromator. Time integrated spectra of the visible emission were recorded on 2" x 11" Tri-X film. Time resolved absolute intensity measurements were made at 4100, 5600, and 6790 A using a monochromator and photomultiplier set to cover a 200 A wavelength interval. The monochromator was calibrated with a tungsten ribbon filament lamp, large enough to fill the optical aperture of the system. An optical pyrometer was used to determine tungsten filament temperature. For control purposes the brightness temperature of the sun was determined on a clear day to be 5600^{o}K.

Shock waves were produced in this tube by a variety of driven section configurations. The largest number of experiments were done using the explosive driver shown in Figure 3(a). A few were done using the transverse explosive driver, Figure 3(b), and the final series used the conventional gaseous combustion driver and diaphragm shown in Figure 3(c).

BLANK PAGE

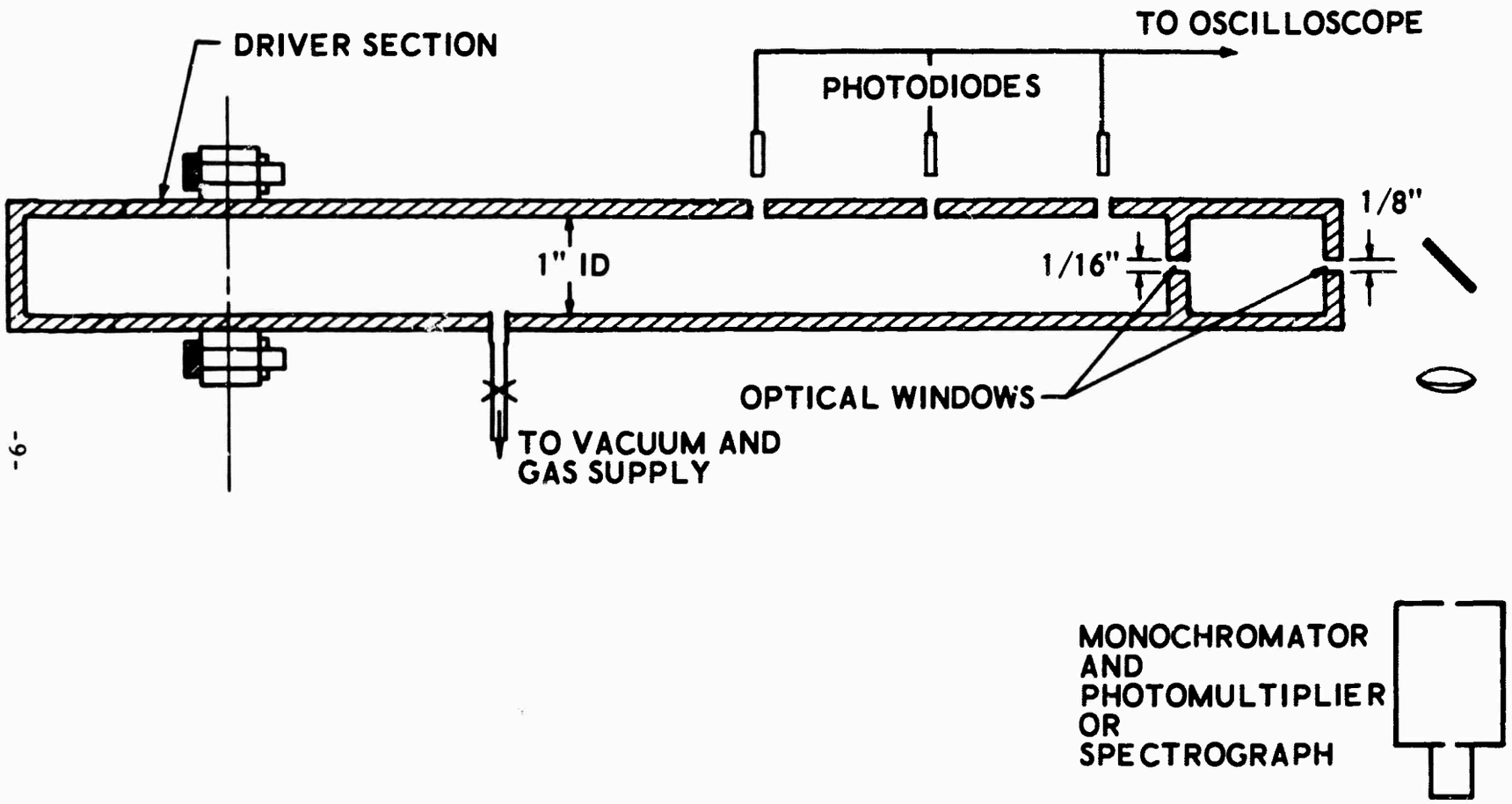

FIGURE 2. CHEMICALLY DRIVEN SHOCK TUBE AND ASSOCIATED INSTRUMENTATION

(a) AXIAL EXPLOSIVE DRIVER

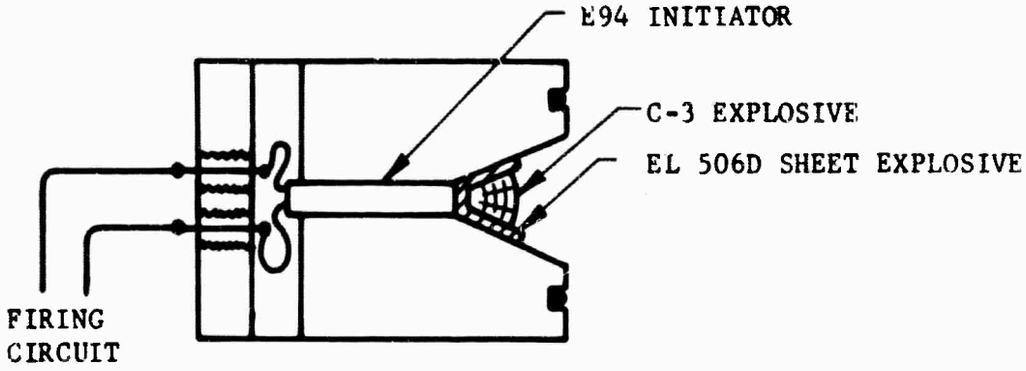

(b) TRANSVERSE EXPLOSIVE DRIVER

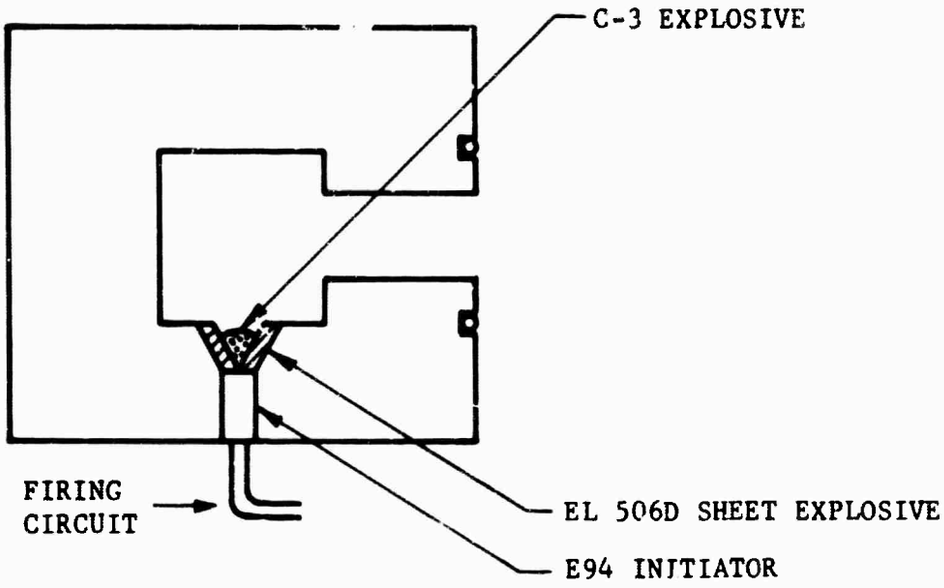

(c) GASEOUS COMBUSTION DRIVER

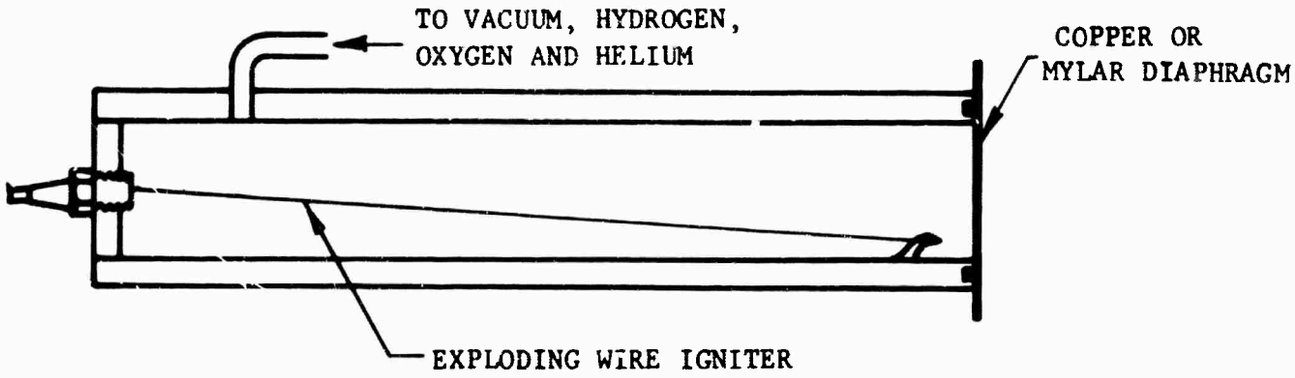

FIGURE 3. LINEAR SHOCK TUBE DRIVER CONFIGURATIONS

A larger shock tube, driven by a hydrogen-oxygen-helium combustion mixture was used for auxiliary experiments. This is a conventional shock tube, 16 feet long with a rectangular 2" x 3" inside cross-section. Photodiodes in the side wall of the tube record the speed of the incident shock wave. Spectral absorption measurements were taken in this tube using a ruby laser light source and two photomultipliers, one to monitor the radiation incident on the test section window, the other to record the radiation transmitted through the test section.

2.3 CONVERSION OF EXPLOSIVE ENERGY TO SHOCKED GAS ENERGY

As the first in a series of energy conversion steps, this process was the first to be evaluated experimentally, utilizing the explosive driver configuration, Figure 3(a). In reducing the experimental data it is helpful to utilize blast wave theory as a guide. The shock speed expected theoretically in an explosively driven linear shock tube can be determined on the basis of conventional one dimensional blast wave theory[2] which yields the relation

$$M_S \approx (\eta E/AN_1 E_1 \ell)^{1/2} \qquad (1)$$

where M_s is the shock Mach number, η the fraction of the total explosive energy, E, transferred to the gas mixture in the tube at the time the shock reaches a point at a distance ℓ from the origin of the blast, A is the cross-sectional area, N_1 the initial number density of atoms, and E_1 the initial gas energy per atom.

From shock speed measurements, a few of which are given in Table 2.1, it was found that the blast wave approximation is applicable if a value $\eta = 0.3$ is used. Detailed comparison between blast wave theory and experiment is shown in Figure 4. Computing the actual gas energy from measured shock speeds it is found to be about 20% of the explosive energy used. No fundamental limitations in this conversion

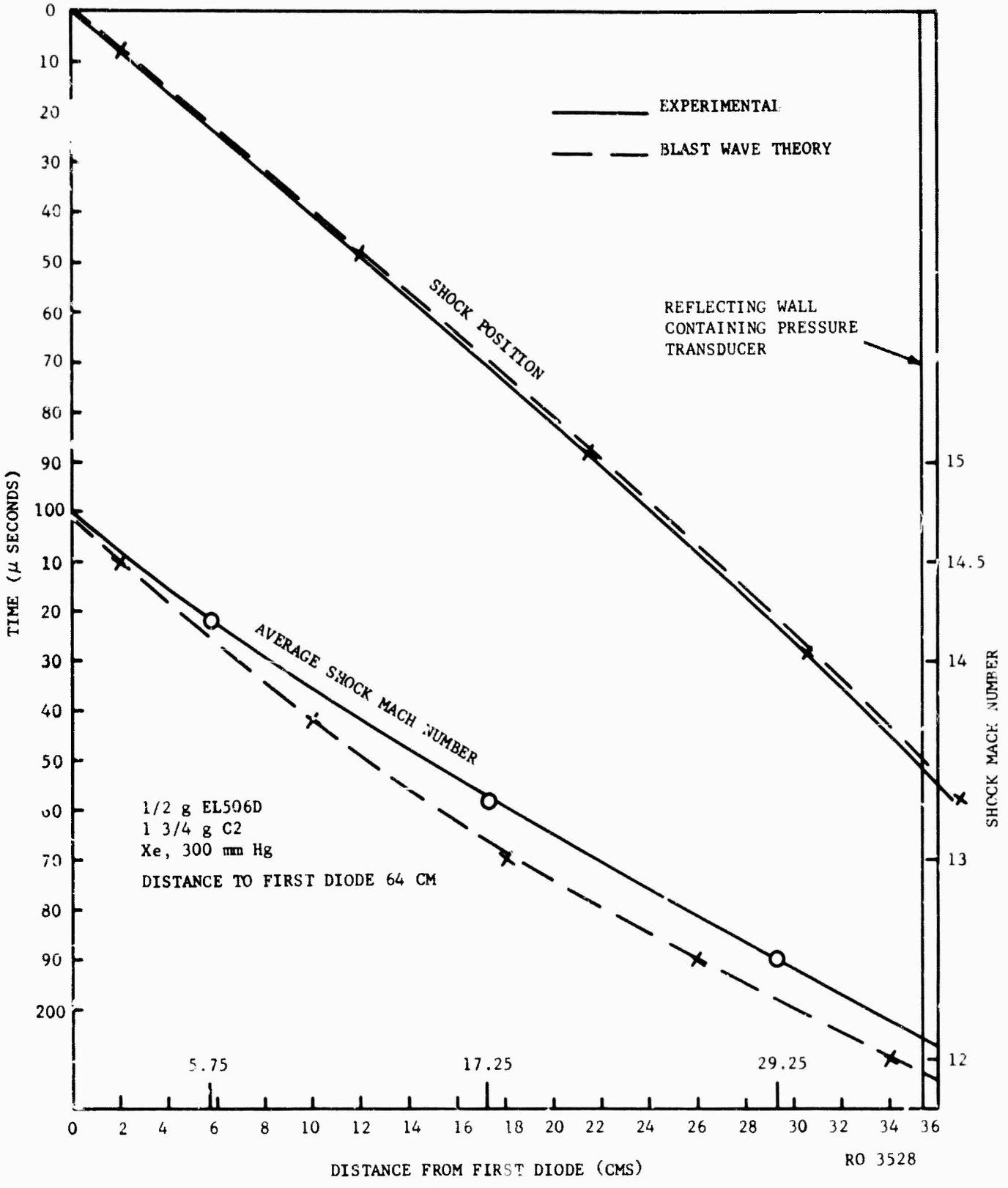

FIGURE 4. SHOCK WAVE POSITION AND SPEED AS A FUNCTION OF TIME, COMPARISON OF EXPERIMENTAL RESULTS WITH BLAST WAVE THEORY

efficiency have been found; with careful design and testing, adequate efficiencies can be obtained. However two basic principles must be recognized in carrying out the design. A high energy conversion efficiency in this step is achieved if the driver gas is expanded by a large pressure ratio, of the order of 10 or more. In addition the final velocity of the driver gas after expansion must be considerably less than the ultimate unsteady vacuum expansion velocity. These two requirements are best met by utilizing a high molecular weight gas such as xenon at low pressures as the driven gas.

TABLE 2.1

RESULTS OF 1 INCH DIAMETER SHOCK TUBE EXPERIMENTS
USING A 2.5 GRAM EXPLOSIVE DRIVER

Tube Length (cm)	Initial Xenon Gas Pressure (mm Hg)	Measured Shock Speed at Far End of Tube (Mach No.)	Theoretical Shock Speed (Mach No.)
100	100	14.6	20
100	100	13.9	20
100	200	12.8	14
100	200	12.8	14
100	400	12.5	10
100	400	11.2	10
100	760	7.8	7
200	100	9.5	14
200	300	7.0	8

2.4 PRESSURE VARIATION WITH TIME

Because expansion waves follow a shock wave driven by an explosive blast, reducing the pressure, gas density, and temperature, it is important to obtain experimental information on the rate of decrease of these parameters. A Kistler 603 piezoelectric pressure transducer was mounted in the reflecting wall of the shock tube and used to record

the time variation of pressure following reflection of the shock wave. The gauge has a natural resonant frequency of about 200 kc and a rise time of 2 μsec.

The oscilloscope records for one experiment are shown in Figure 5, in addition to the record of arrival time of the incident shock wave at the 3 diodes. The measured incident shock speed extrapolated to the reflecting wall corresponds to Mach number 12.1. The theoretical pressure behind the reflected shock at $M_s = 12.1$ and an initial xenon pressure of 300 mm Hg is 6400 psi, which agrees within experimental uncertainty with the measured peak pressure of 7000 psi. Unfortunately, the ringing response of the pressure transducer obscures the details of the pressure variation with time, but it can be seen that the e-folding decay time in pressure is about 200 μsec. Two additional pressure increases at about 200 μsec and 450 μsec after shock reflection are noted, but are not of sufficient magnitude to change the properties of the gas significantly.

The energy loss associated with this pressure drop is evaluated in Section 2.8 and shown to be an insignificant energy loss mechanism.

2.5 CONTINUUM ABSORPTION MEASUREMENTS

The use of the Kramers-Unsold theory for continuum emission in argon has been verified experimentally[3,4] at electron densities of the order of 10^{17} cm^{-3}, but not at the high values of electron density ($\sim 10^{19}$) currently used in the explosively shocked radiation source. Because this theory must be used in evaluating the spectral measurements, verification of the theory at these high electron densities was necessary. An auxiliary experiment was carried out in the 2" x 3", 16' long, rectangular shock tube, to measure the absorption coefficient of shock heated argon at electron densities as high as 1.9×10^{18} cm^{-3}. This high electron density is produced behind the reflected shock, driven by a helium, hydrogen, oxygen

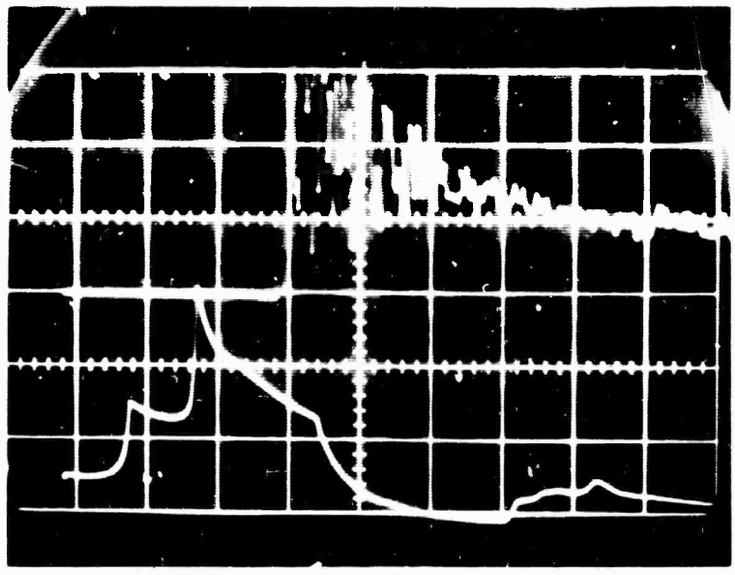

(a) 50 μSEC/cm SWEEP. UPPER BEAM 1v/cm, PRESSURE TRANSDUCER. LOWER BEAM 20 v/cm, SHOCK TIME.

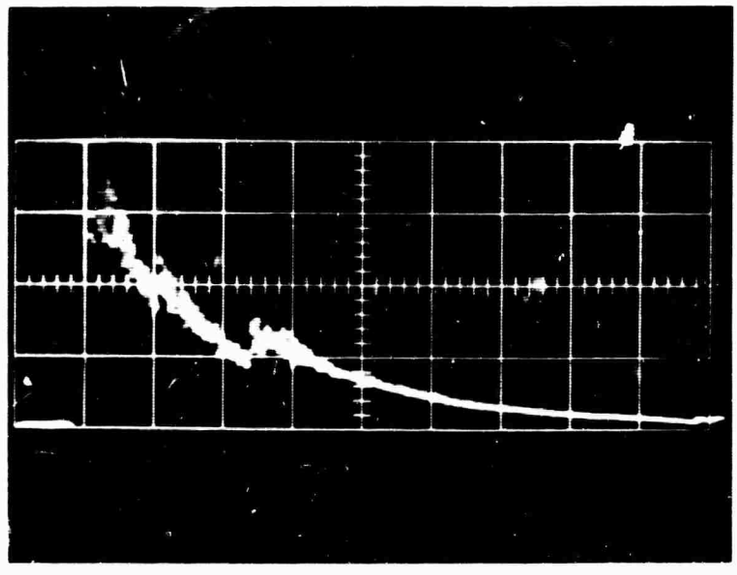

(b) 200 μSEC/cm SWEEP. 0.5v/cm, PRESSURE TRANSDUCER.

R03526

FIGURE 5. OSCILLOSCOPE RECORDS OF THE GAS PRESSURE AT THE REFLECTING WALL OF THE EXPLOSIVELY DRIVEN XENON SHOCK TUBE. ALSO SHOWN IS A RECORD OF SHOCK ARRIVAL TIME AT STATIONS 4.5" APART.

combustion mixture ignited by a thin nichrome exploding wire located along the central axis of the driver section. The absorption coefficient of the shock heated gas is determined by comparing the intensity of light from a pulsed ruby source transmitted through the shock tube to that directly from the source. The speed of the incident shock wave is recorded by the response of semiconductor photodiodes to the luminosity behind the incident shock wave.

The experimental measurements shown in Figure 6a were made using argon at an initial pressure of 3 cm Hg in which an incident shock Mach number of 11.0 was recorded. The reflected shock passed the light beam at the time, t_r, shown by the vertical line on the film. Prior to this time no detectable absorption was recorded, the theoretical value of the attenuation being 7% behind the incident shock. Considerable attenuation was recorded following passage of the reflected shock and it is seen that the attenuation decreases quite rapidly with time after reaching its maximum value. Quantitative reduction of the data (shown in Figure 6b, where the ratio of incident intensity, I_o, to transmitted intensity I, is given) was accomplished by comparing amplitudes of the laser spikes, providing accurate time correlation of the transmitted and the direct beam records.

At time t = 0, the time of passage of the reflected shock through the beam, the predicted Kramers-Unsold absorption[5] at this wavelength (6935A) is shown assuming equilibrium conditions and no radiation cooling behind the reflected shock. The data extrapolated to t = 0 (there were no laser spikes in the time interval 0 to 8 μsec) falls somewhat below the theoretical value, but lies within the bounds set by uncertainties in the experiment.

A qualitative radiation cooling theory was formulated assuming blackbody radiation energy loss from the shock heated gas between the light beam and the reflecting wall (a distance of 3.5 cm) to the half plane of the end wall of the shock tube. A constant pressure process

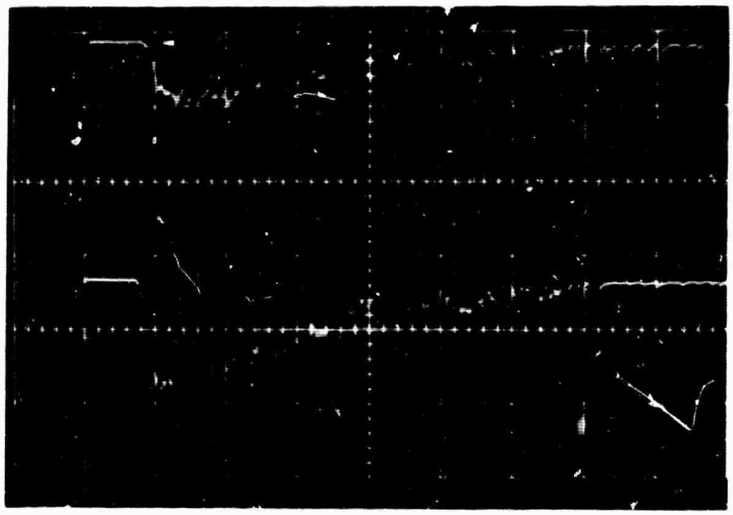

FIGURE 6a. OSCILLOSCOPE RECORDS OF LASER BEAM ATTENUATION BY OPTICALLY THICK ARGON PLASMA. 3 cm Hg INITIAL PRESSURE, M_S = 11, SWEEPSPEED 50 μSEC/cm, 0.5 v/DIVISION. UPPER BEAM IS LASER SOURCE MONITOR. LOWER BEAM IS A MONITOR OF LASER LIGHT TRANSMITTED THROUGH THE SHOCK TUBE, SHOWING ATTENUATION ABRUPTLY AT 360 μ SEC AFTER BEGINNING OF THE TRACE.

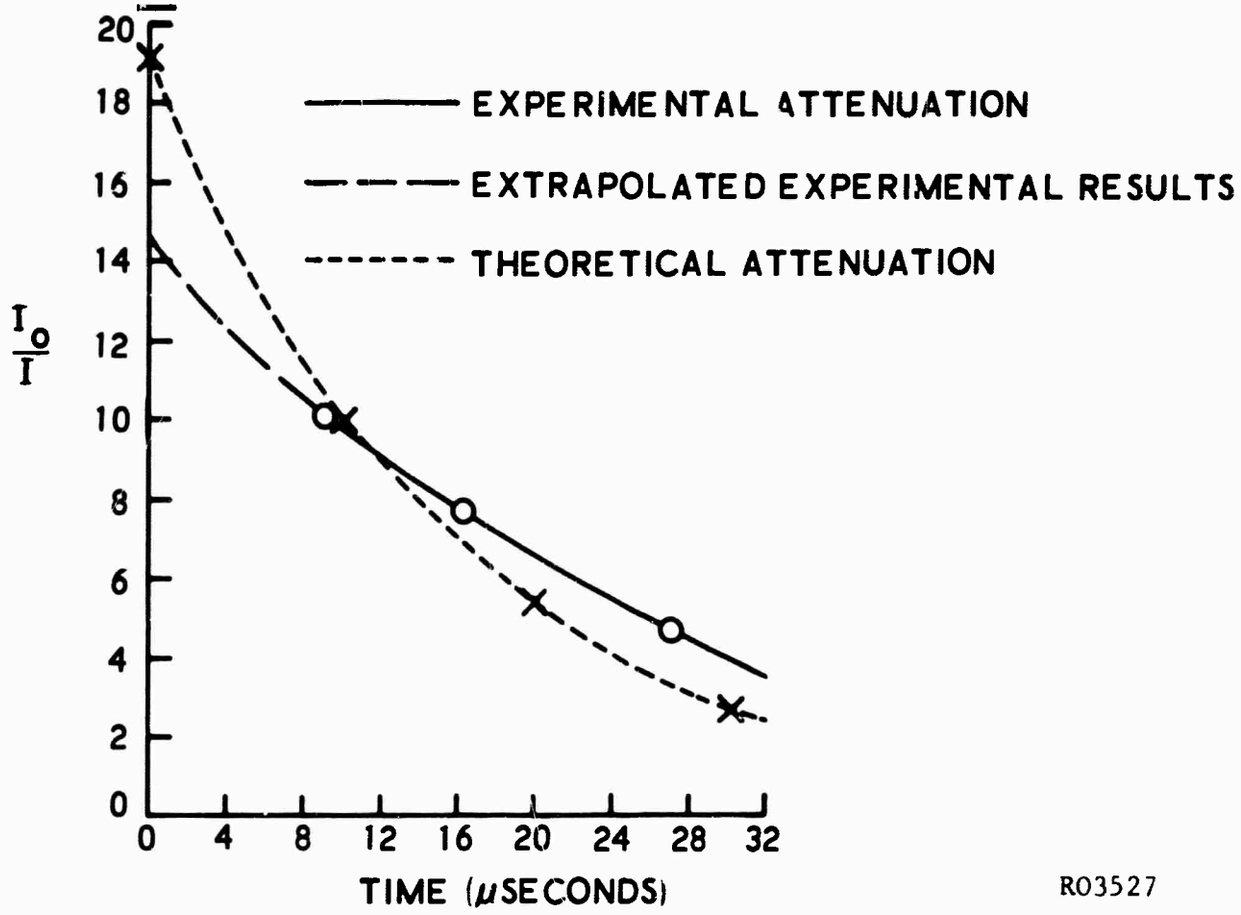

FIGURE 6b. RATIO OF UNATTENUATED BEAM INTENSITY TO INTENSITY RECORDED AFTER PASSING THROUGH REFLECTED SHOCK HEATED ARGON IN THE 2" X 3" SHOCK TUBE

was assumed with the electron density in equilibrium with the changing gas temperature. The theoretical cooling curve is shown in Figure 6b, and is in fairly good agreement with experiment.

The rapid cooling of the gas probably results in a lower initial value of I_o/I due to the finite width of the light beam. The width of the beam is 1 cm, requiring about 9 μ secs for passage of the reflected shock from one edge of the beam to the other. During the first 9 μsecs the theoretical attenuation falls by a factor of about 2, and will produce a smaller initial I_o/I by a factor of the order of 1.5. This is approximately the discrepancy between the initial value obtained experimentally and that computed from Kramers-Unsold theory.

Thus the use of the Kramers-Unsold expression is verified by this experiment for optically thick conditions and is justified in the theoretical analysis of the explosively shocked radiation source. In addition the qualitative model for radiation cooling is verified and can be extrapolated to higher densities with reasonable certainty.

The time for this gas to cool to optically thin conditions is about 30 μsec. This time is roughly proportional to the initial gas density and is also proportional to the ratio of gas volume to radiating surface area. This observed decay rate, found in the large shock tube at an initial argon pressure of 3 cm Hg and an initial shock Mach number of 11, can be extrapolated to the conditions of the small explosively driven shock tube at an initial xenon pressure of 30 cm Hg and an initial shock Mach number of 13. Thus if there were no decay due to expansion waves (i.e., constant speed incident shock throughout the length of the explosively driven shock tube) the time required for the gas to decay by radiation losses to an optically thin plasma would be greater than 200 μsec, considerably longer than the 50 μsec time observed experimentally.

2.6 SPECTRAL MEASUREMENTS

A Cenco grating spectrograph was used to observe the time integrated visible spectrum emitted by the explosively shocked xenon radiation source. Light from a 1/16" optical aperture covered by a lucite window in the end wall of the explosively driven shock tube, transmitted through a 1/8" aperture, 1/2" away, and focused on the entrance slit of the spectrograph, was recorded on 2" x 11" Tri-X film. The spectrum, shown in Figure 7, is seen to be continuous over the wavelength range from 4000 to 7000 A, except for a fairly broad ($\sim$14 A) absorption line at about 5300 A. This line is tentatively identified as the 5330 A absorption line ($3p\ ^5P$ to $5d\ ^5D^o$) of atomic oxygen, which is a product of ablation of the lucite window. The gaseous products of ablation at temperatures sufficiently high to produce appreciable absorption are C, CO, O, and H. The nearest xenon emission lines are rather weak at 5248 A and 5393 A. From this experimental information it is verified that the radiation spectrum is continuous as expected under these gas density and temperature conditions, with the principal radiation coming from free-free transitions (Bremsstrahlung) and free-bound transitions of electrons in the field of xenon ions.

Using the monochromator described in Section 2.2, time resolved absolute spectral measurements were taken at 4100 A, 5600 A, and 6790 A, using a 200 A bandwidth. Results from several typical experiments, given in terms of brightness temperature, are shown in Figures 8, 9, 10, and 11. Shock speeds (given in terms of the cold flow Mach number in shock fixed coordinates) for these runs are shown in Figure 12. For comparison the surface brightness of a single linear xenon flash lamp, unclad and supplied by 50 joules of electrical energy is shown in Figure 8.

RO3531

FIGURE 7. TIME INTEGRATED SPECTRUM OF THE EMISSION THROUGH A LUCITE WINDOW IN THE END WALL OF THE SHOCK HEATED XENON RADIATION SOURCE. INITIAL GAS PRESSURE 300 mm Hg, 1 GM EL 506D AND 3.5 GM C2 EXPLOSIVE CHARGE. CADMIUM DISCHARGE LAMP USED FOR WAVELENGTH CALIBRATION.

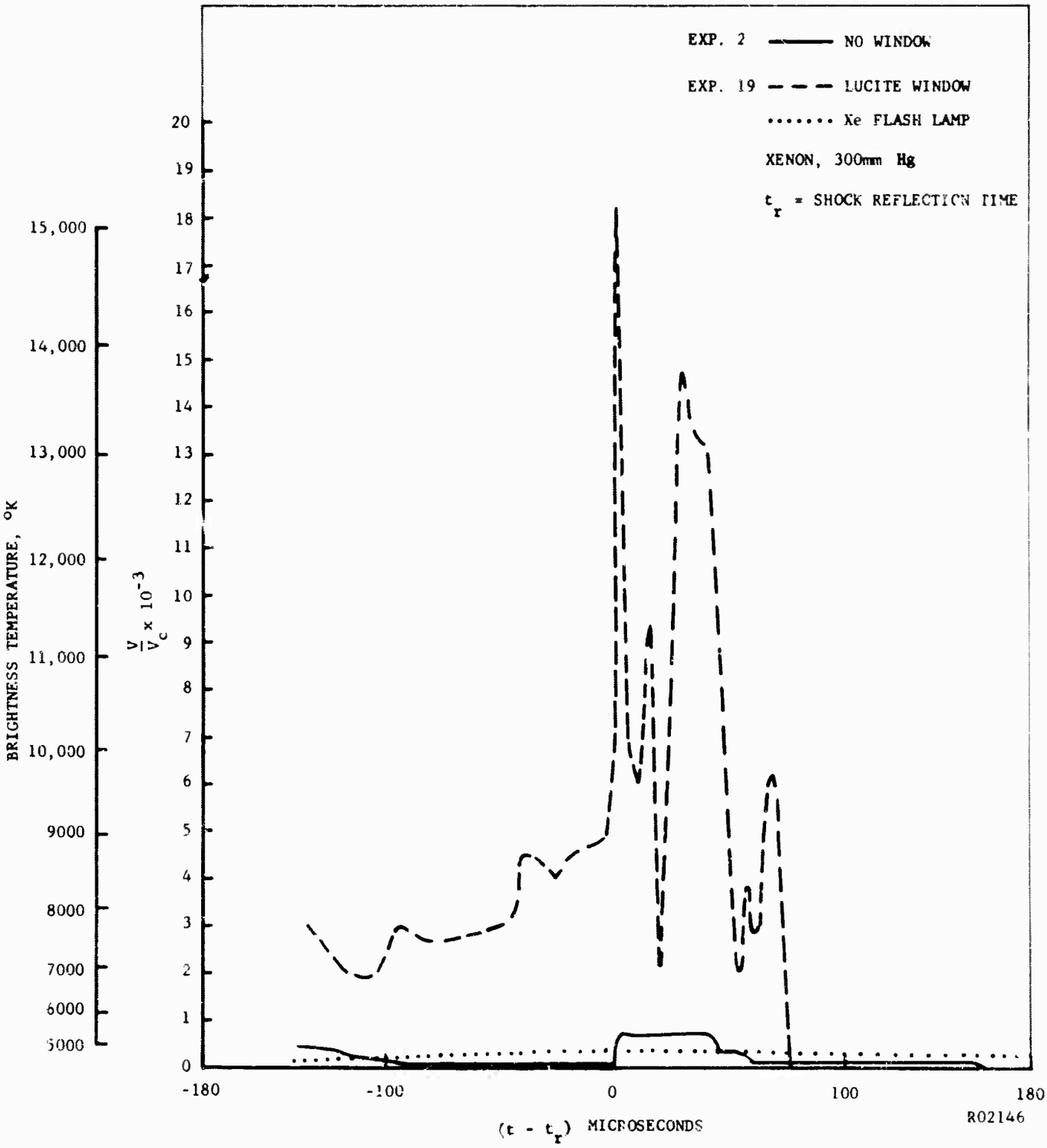

FIGURE 8. SPECTROMETER RESPONSE (5600 ± 110A) TO SHOCK RADIANCY, V, RELATIVE TO TUNGSTEN LAMP RADIANCY, V_c, AT 2273°K, USING THE AXIALLY DIRECTED EXPLOSIVE DRIVER CONFIGURATION

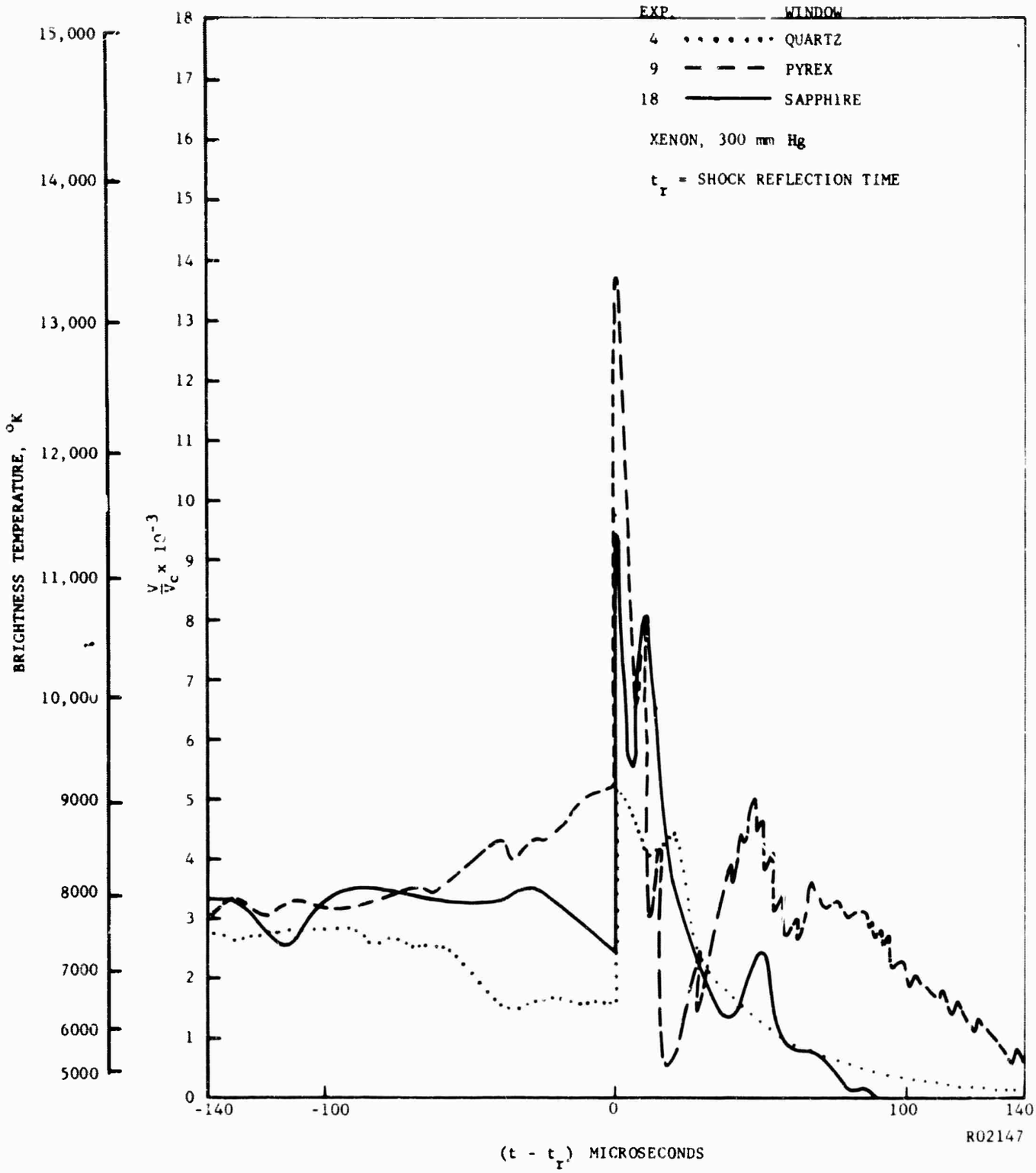

FIGURE 9. SPECTROMETER RESPONSE (5600 ± 110A) TO SHOCK RADIANCY, V, RELATIVE TO TUNGSTEN LAMP RADIANCY, V_c, AT 2273°K, USING THE AXIALLY DIRECTED EXPLOSIVE DRIVER CONFIGURATION

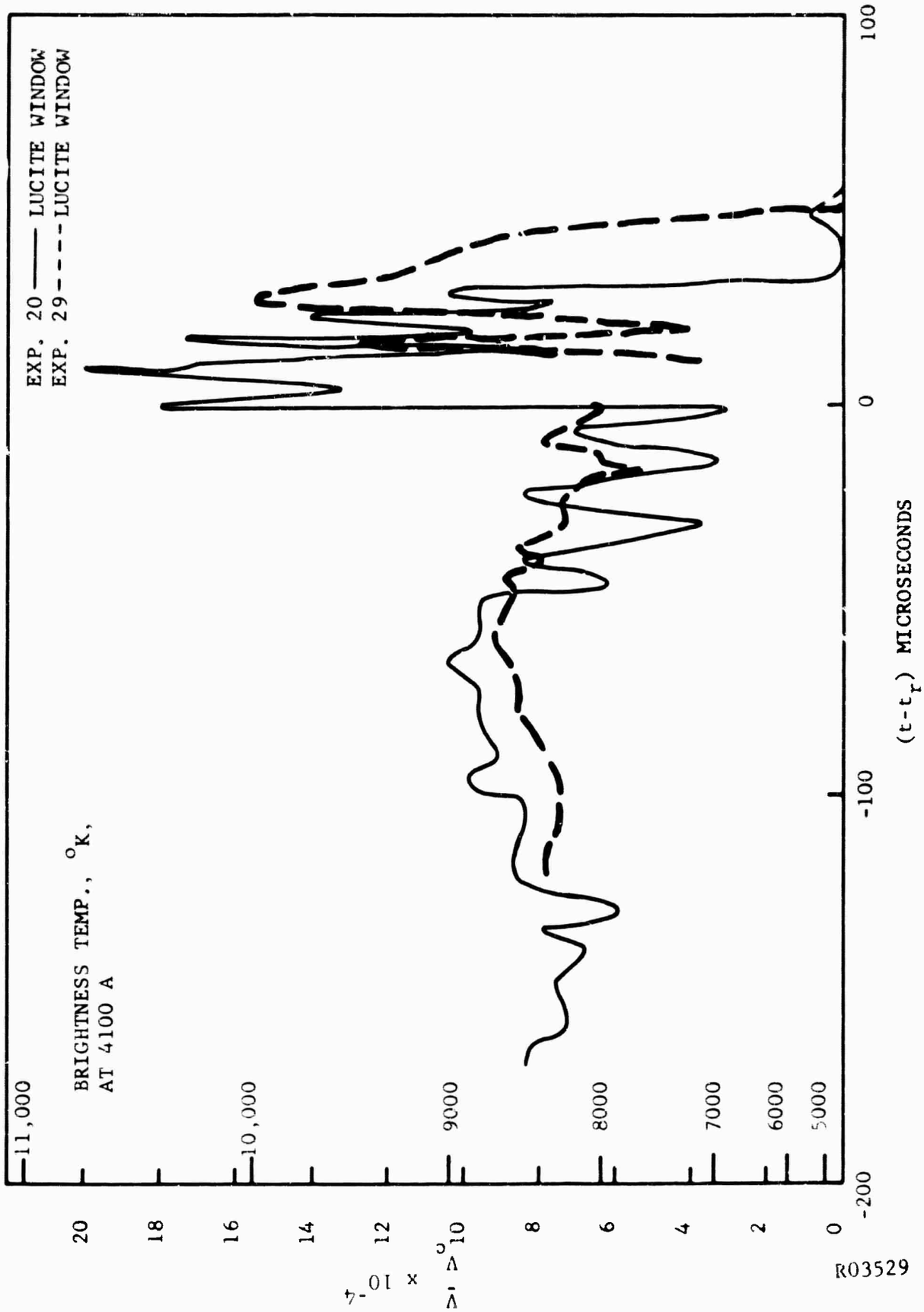

FIGURE 10 SPECTROMETER RESPONSE (4100A, 220A BANDWIDTH) TO SHOCK RADIANCY,V, RELATIVE TO TUNGSTEN LAMP RADIANCY,V_c, AT 2273°K, USING THE AXIALLY DIRECTED EXPLOSIVE DRIVER CONFIGURATION

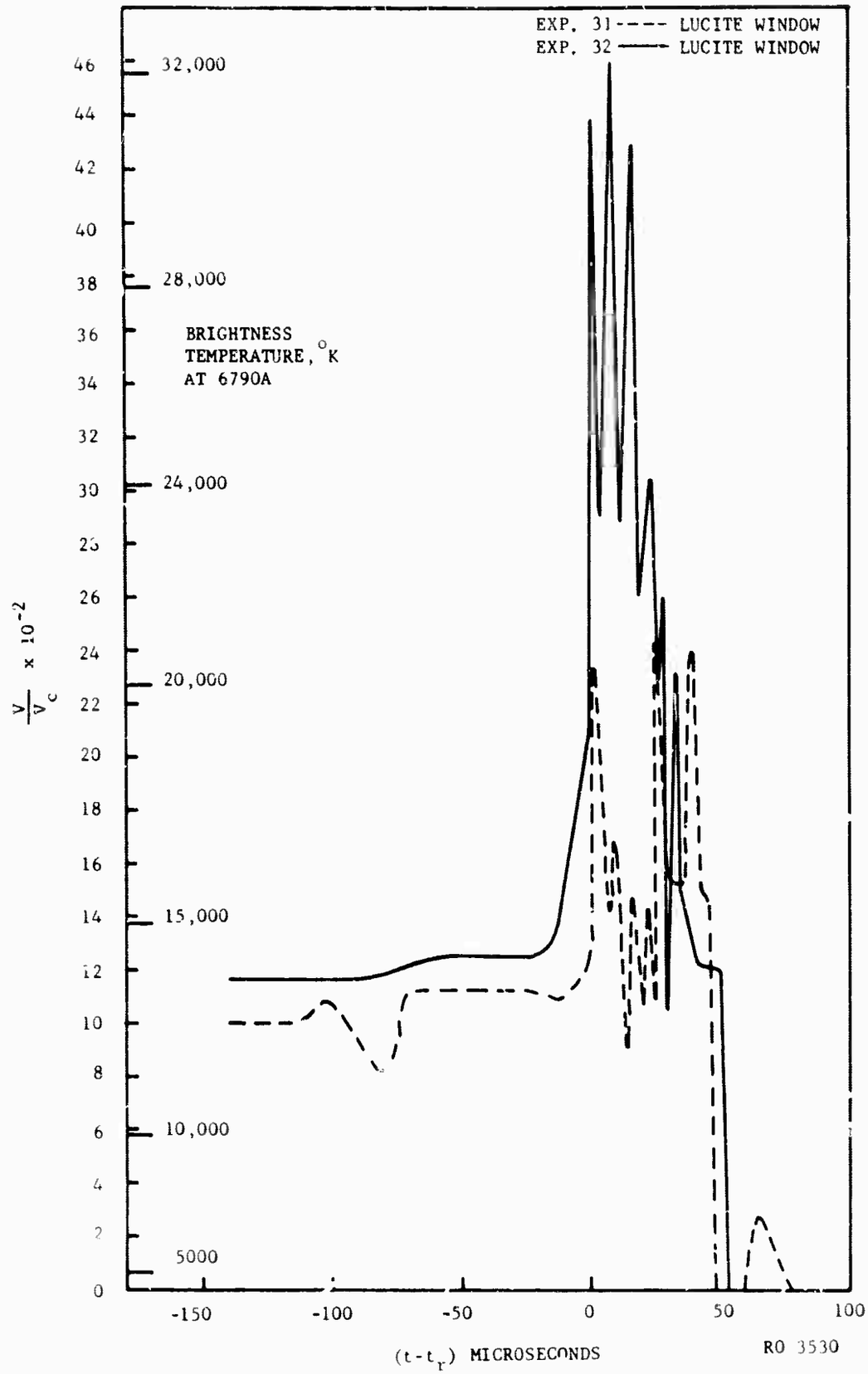

FIGURE 11. TIME RESOLVED MONOCHROMATOR RESPONSE OF THE SHOCKED XENON RADIATION SOURCE AT A WAVELENGTH OF 6790A (200A BANDWIDTH), USING THE AXIALLY DIRECTED EXPLOSIVE DRIVER CONFIGURATION

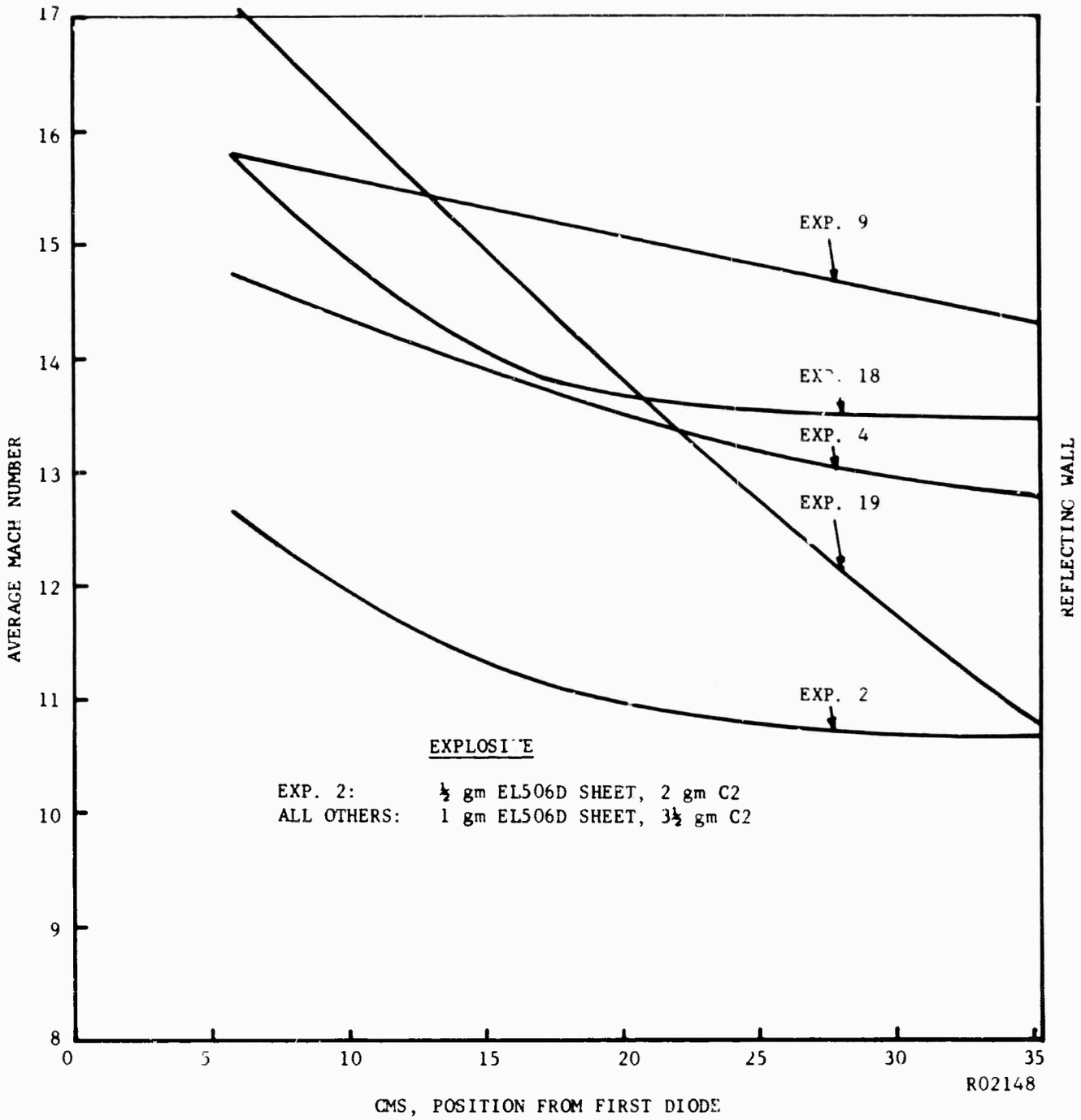

FIGURE 12. AVERAGE INCIDENT SHOCK MACH NUMBER VERSUS POSITION IN SHOCK TUBE FOR EXPERIMENTS USING THE AXIALLY DIRECTED EXPLOSIVE DRIVER CONFIGURATION

Comparing Exp. 2 with 19, it is seen that the weaker shock (Exp. 2) results in much lower luminosity behind the incident shock. This is because the incident shock Mach number is only about 11, insufficient to produce an optically thick plasma. Increasing the amount of explosive by 80% (Exp. 19) resulted in a 30 fold increase in incident shocked gas luminosity. Using the larger explosive charge, the surface brightness of the incident shocked gas lies consistently between 7000°K and 9000°K, approaching the equilibrium gas temperature ($\sim$11,000°K).

The surface brightness of the gas heated by both the incident and the reflected shock wave was recorded with several window materials as well as no window at all. The no window results are not very reproducible, but do show consistently lower peak brightness temperatures than those recorded with windows in place. This, together with the rapid rise in luminosity at the time of reflection ($\sim$5 μsec), indicates, as expected, that the optical depth of the shock heated gas is less than several times the diameter of the viewing hole, i.e., less than 5 mm.

Behind reflected shocks with windows in place, brightness temperatures as high as 15,000°K were recorded at 5600 A, comparable to expected equilibrium gas temperatures. The duration of useful radiation from the reflected shock heated gas is 60 μsec or less, considerably shorter than expected.

The investigation of wall materials included pyrex, fused quartz, and synthetic sapphire, each exhibiting a roughly exponential decay in radiation, having a decay time of about 25 μsec (see Figure 9). Lucite window material, on the other hand, transmitted high luminosity for 50-60 μsec, resulting in 2 to 3 times greater total energy radiated (Figure 8). Noticeable ablation of the lucite windows is indicated by the rounded, clear, fire polished appearance of the surface following the experiments. In addition, because of the ablation blanket, there is little deposition on these windows of solid products produced in the experiment.

Absolute spectral measurements at 4100 A and 6790 A are shown in Figures 10 and 11. The peak brightness temperature at 4100 A was 9000°K to 11,000°K, somewhat lower than that of 15,000°K observed at 5600 A. However at 6790 A, the peak brightness temperatures range between 22,000°K and 32,000°K, considerably higher than the computed equilibrium gas temperature. This result, which can arise only from some non-equilibrium process, was completely unexpected at the high densities produced in the reflected shock heated gas. The atom densities are of the order of 10^{20} cm^{-3}, with corresponding collision frequencies of 10^{10} sec^{-1}. Collision frequencies for electronic excitation and de-excitation by electron impact are also of the order of 10^{10} sec^{-1} under equilibrium conditions behind the reflected shock. With such high collision frequencies it is difficult to imagine a mechanism which can distort the expected Maxwell-Boltzmann distribution of velocities and excited state populations and produce radiation intensities in the red region greater than local blackbody values.

Subsequent experiments, described below, indicated that explosive products actaully penetrated the reflected shock heated xenon region. From this it may be postulated that unburned explosive products mixing with the hot xenon are ignited, producing chemiluminescent radiation in the red wavelength region. However since we have no further experimental information which has a bearing on this speculation no definite conclusions can be drawn at this time regarding the source of this unexpected effect.

2.7 TRANSVERSE EXPLOSIVE DRIVER EXPERIMENTS

Because of the large fluctuations in intensity and the lack of reproducibility of results from one experiment to the next it was thought that a portion of the explosive or the explosive products may be mixing with the shock heated xenon. These impurities may lower the gas temperature,

thus lowering the intensity at 4100 A, but, through chemiluminescence may produce higher than blackbody radiation in the red portion of the spectrum. Additional mixing of more inert material from the explosion may be the cause of the short radiation pulse duration.

To test this idea the explosion was directed transverse to the shock tube axis leaving any unburned explosive products or inert products in a small cavity recessed one inch below the inside surface of the tube (see Figure 3(b)). The change in the character of the results was striking as can be seen by comparing Figure 13 with Figure 8. The duration increased somewhat, good reproducibility was achieved, fluctuations in intensity almost disappeared, and the unexpectedly high intensity at 6790 A was replaced by more reasonable intensities (see Figure 14). It is concluded from these experiments that mixing of explosive products with the shock heated xenon was a significant problem, and represents a fundamental limitation in exploiting radiation from explosively driven reflected shock heated gases.

Using the transverse directed explosive configuration the change in intensity and pulse duration with change in initial xenon pressure was also studied. Three causes for the short experimental pulse duration have been considered: (1) radiation cooling, (2) quenching by mixing with explosive products, and (3) absorption in the cool ablation boundary layer. If the pulse duration is limited either by (1) or (2), it will increase with increasing xenon pressure. If it is limited by (3) it will decrease with increasing pressure.

Experimentally (Figure 15) it was found that the pulse duration increases almost linearly with increasing pressure, showing quite conclusively that window ablation is not a significant limiting factor. However the sudden quenching of radiation at 50 to 100 μsec was still present. To determine whether the cause was radiation cooling or quenching by mixing with explosive products the analysis described in the next section was carried out.

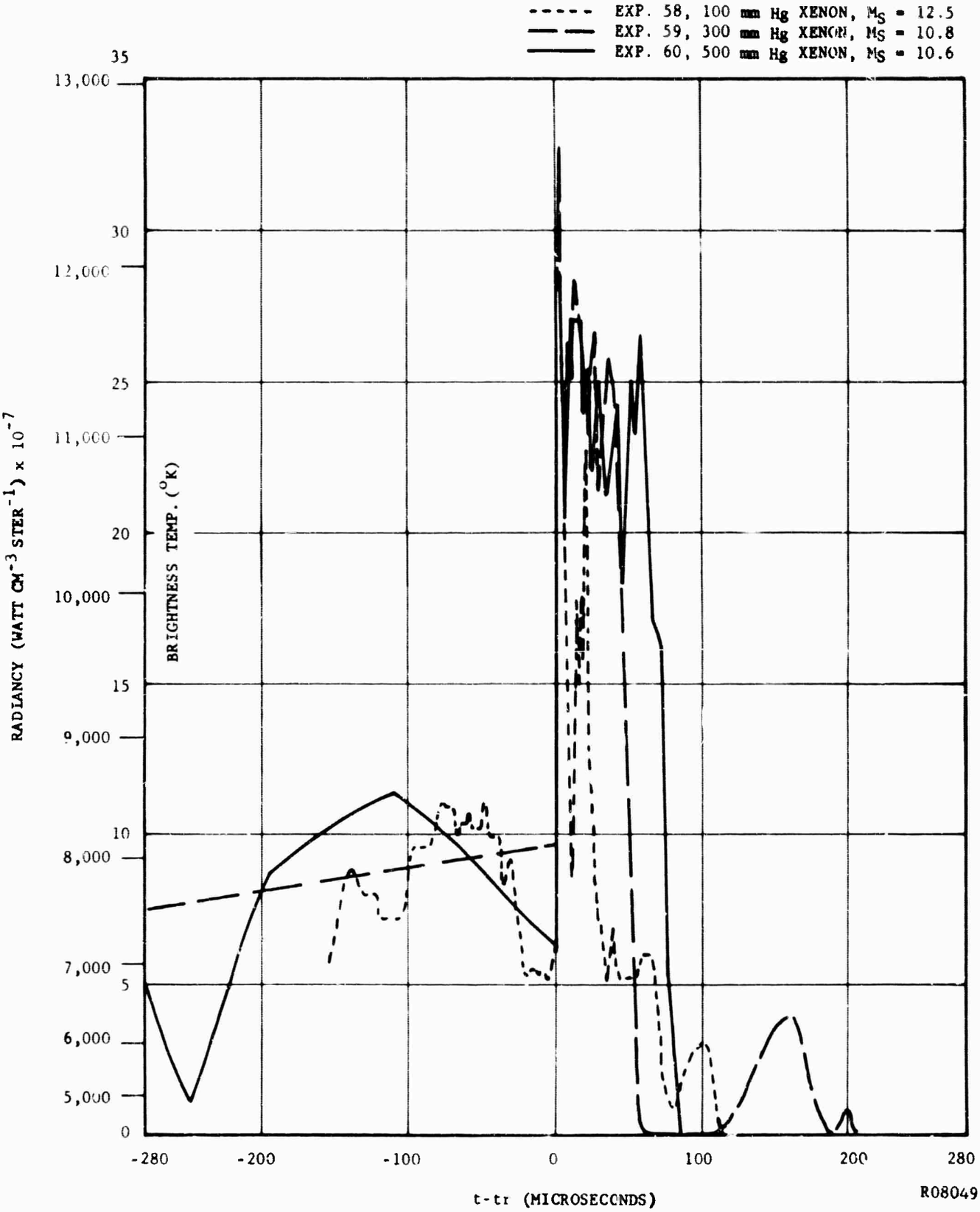

FIGURE 13. REFLECTED SHOCK RADIANCY VERSUS REFLECTED SHOCK TIME USING THE TRANSVERSE EXPLOSIVE DRIVER CONFIGURATION (5600A, 22[illegible] BANDWIDTH)

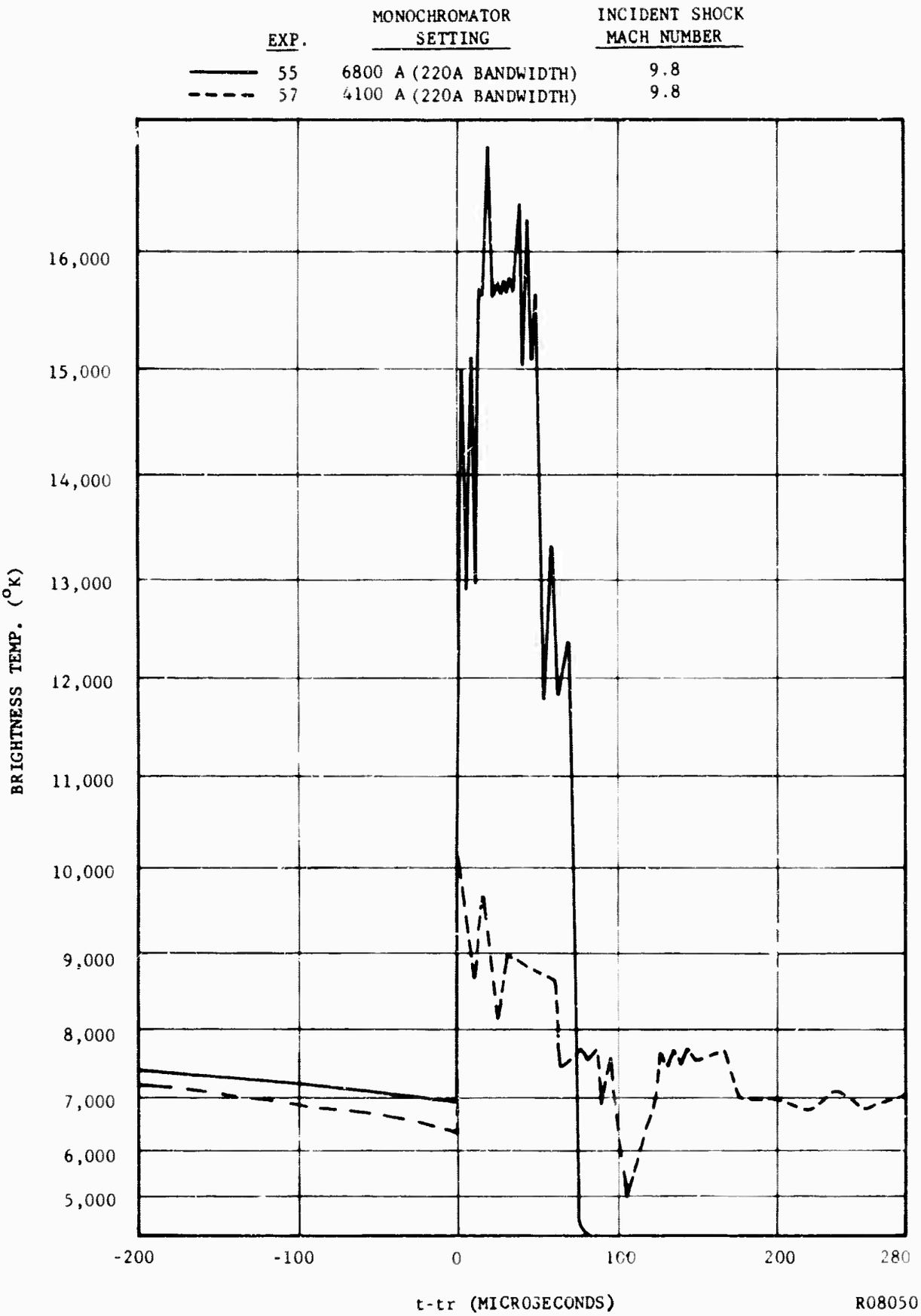

FIGURE 14. REFLECTED SHOCK BRIGHTNESS TEMPERATURE VERSUS TIME USING THE TRANSVERSE EXPLOSIVE DRIVER CONFIGURATION AND 300 mm Hg INITIAL XENON PRESSURE

2.8 ANALYSIS OF GAS COOLING BY RADIATION AND EXPANSION WAVES

For comparison with the time resolved spectral measurements, a quantitative analysis of the temperature-time history of the reflected shock heated gas was formulated, taking into account both radiation cooling and expansion cooling. From Figure 4 it is seen that the behavior of the incident shock wave is very close to that predicted by one dimensional blast wave theory, a theory which will be useful in further analysis of the data. With this information on the shock speed decay rate and the previously described information on pressure decay, together with the observed radiative emission, it will be possible to determine theoretically the change in gas properties with time Since the radiation is observed to decay sharply at 50 μsec, we naturally ask if this is the time at which the gas becomes optically thin due to these energy losses. To answer this, the gas properties are computed at the reflecting wall after 50 μsec and at the position of the reflected shock at this same time.

At the reflecting wall the loss of gas enthalpy by radiation and by pressure drop is given by[6]

$$dH = dQ_{rad} + \frac{dp}{\rho} \qquad (2)$$

or in integral form, assuming $p \propto \rho$ (high specific heat)

$$H - H_o = Q_{rad} + RT_o(1 + \alpha_o) \ln (p_o/p) \qquad (3)$$

The energy radiated is assumed to be that of a blackbody at the equilibrium gas temperature, roughly 15,000°K. Although the experimental measurements indicate lower radiation in the violet and greater in the red, this is a good approximation for the total emission. Also as a first approximation the internal radiative heat transfer is assumed rapid enough to cause the radiating gas to lose energy uniformly. Then

$$Q_{rad} = \int_{t_o}^{t} \frac{\sigma T^4}{\rho V} A_s \, dt \qquad (4)$$

where σ is the Stefan Boltzmann constant, A_s the radiating surface area, and V the gas volume at time t.

$$A_s = \pi D^2/2 + \pi Dx, \quad V = \pi D^2 x/4 \qquad (5)$$

Since the reflected shock position, x, is given by $x = U_r t$ where U_r is nearly constant and equal to about 1/3 U_s, equation (4) becomes

$$Q_{rad} = \int_{t_o}^{t} \frac{\sigma T^4}{\rho} \left(\frac{\pi D^2/2 + \pi Dx}{\pi D^2 s/4}\right) dt$$

$$\sim \frac{2\sigma T^4}{\rho}\left[\frac{1}{U_r} \ln \frac{t}{t_o} + \frac{2}{D}(t - t_o)\right] \qquad (6)$$

where t_o is the time after shock reflection at which the gas first becomes optically thick (about 2 μsec). Substituting numerical values of $T = 15{,}000^{\circ}K$, $\rho = 1.3 \times 10^{20}$ particles/cm^3, $U_r = 7 \times 10^4$ cm/sec, D = 2.5 cm, and t = 50 μsec, $Q_{rad} \approx 2.3$ electron volts/atom for the gas at the reflecting wall.

Now the pressure ratio p_o/p determined experimentally 50 μsec after shock reflection is approximately 1.3. The term $RT_o (1 + \alpha_o) \ln p_o/p$ is thus approximately 0.45 ev/atom. The initial enthalpy of the gas, $H \simeq U_s^2$, at an incident shock Mach number of 13 in xenon is 7.5 ev/atom. Thus after 50 μsec the enthalpy of the gas at the reflecting wall is roughly 4.7 ev/atom.

The degree of ionization at this enthalpy level and density is 10%. The atom density drops directly with pressure from 2 x 10^{20} cm^{-3} behind the reflected shock to 1.5 x 10^{20} cm^{-3}. Thus the electron density is about 1.5 x 10^{19} cm^{-3} for which the optical depth is about 0.5 mm, considerably smaller than the dimensions of the shock heated gas. The optical depth is computed from the results of Pomerantz[5] and is inversely proportional to the square of the electron density. The variation of the linear absorption coefficient with temperature and wavelength at an electron density of 10^{19} cm^{-3} is shown in Figure 15.

Similarly it can be shown that the gas at the position of the reflected shock 50 μsec after reflection has an optical depth of about 2 mm. The enthalpy and density of this gas are considerably lower than those of the gas at the reflecting wall, due to the expansion waves. The reflected shock travels some 4 cm in 50 μsec, a point at which the gas density, prior to the compression by the reflected shock, is only 2.5 x 10^{19} cm^{-3}, a factor of 2.5 less than that after compression by the incident shock. This is obtained from blast wave theory, using a constant specific heat ratio of 1.4.[2] The enthalpy of the gas is reduced to approximately 65% of the initial enthalpy of the gas at the reflecting wall, or 4.9 ev/atom. This arises because of the decay in static enthalpy and flow velocity of the gas caused by expansion waves prior to arrival of the reflected shock. Thus the electron density at this point is 6 x 10^{18} cm^{-3}, resulting in an optical depth in the visible of about 2 mm, much smaller than the gas thickness of 4 cm.

If 100 μsec is allowed for radiation cooling and pressure decay the gas enthalpy at the reflecting wall drops to 3.2 ev/atom, the electron density to 4 x 10^{18} cm^{-3}, and the optical depth increases to 5 mm. At about 150 μsec the gas gradually becomes optically thin, and the radiation intensity decreases with a time constant of 100 to 200 μsec rather than the abrupt decrease observed experimentally.

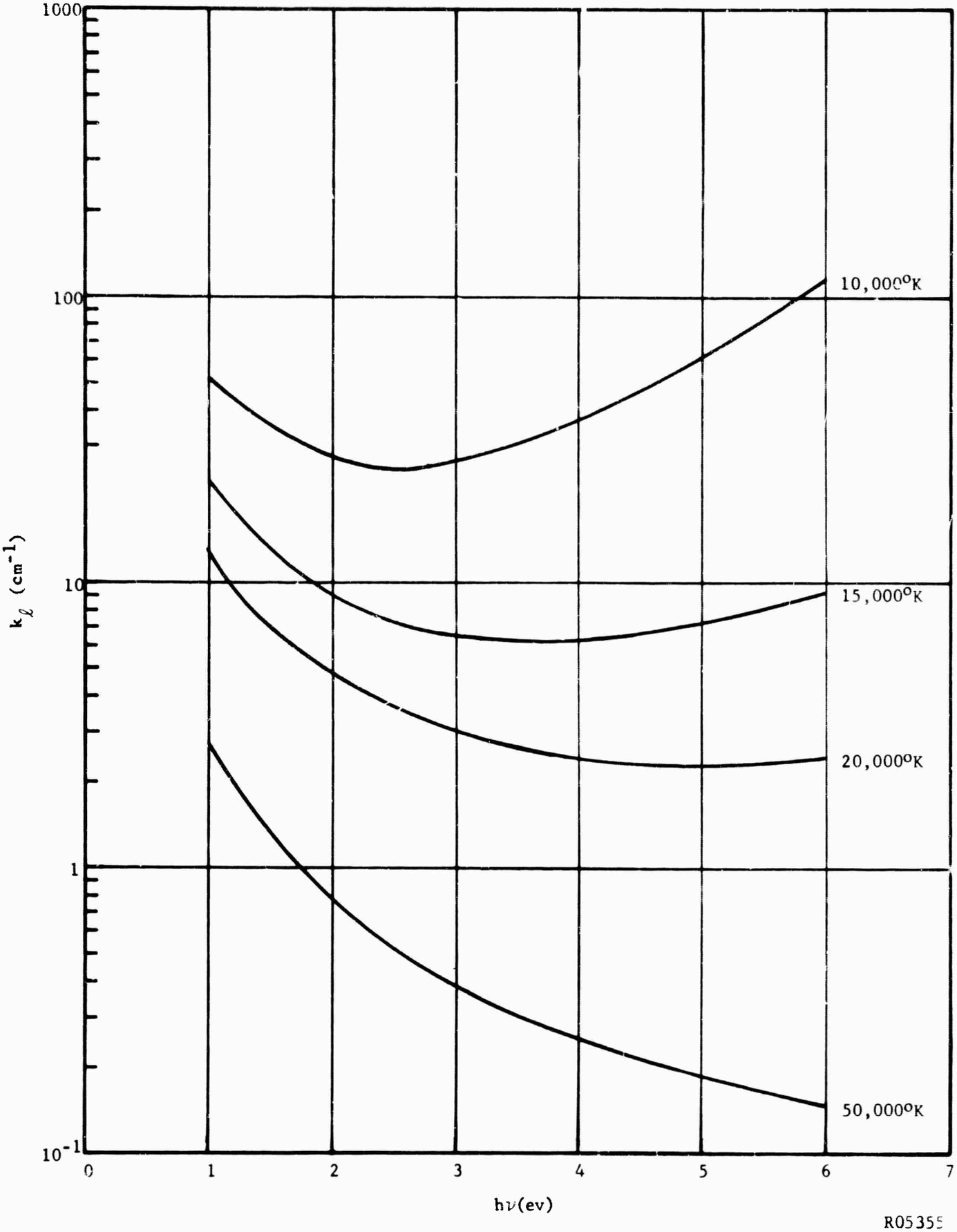

FIGURE 15. THEORETICAL FREE-FREE AND FREE-BOUND ABSORPTION COEFFICIENT AT AN ELECTRON DENSITY OF 10^{19} CM^{-3}

It is concluded from this analysis that some process other than radiation cooling and expansion wave losses is responsible for the sudden quenching of radiation at 50 μsec after shock reflection. It has already been shown (Section 2.6) that this quenching is not a result of window ablation or gas cooling by heat conduction to the wall. The evidence described thus far points strongly toward mixing of the colder explosive products with the high temperature shock heated xenon, resulting in premature quenching.

2.9 GASEOUS COMBUSTION DRIVER EXPERIMENTS

This premature quenching was the most severe limitation encountered in the program, requiring further study to ascertain the exact cause of the effect. Because even the transverse explosive driver produced some solid particle material, the source of the quenching was thought to be the intrusion of solid particles into the gaseous reflected shock heated xenon region. To eliminate solids a gaseous combustion driver (Figure 3(c)) was fitted to the shock tube. This driver was filled with 35 psia partial pressure O_2, 55 psia H_2, and 145 psia He, and ignited by exploding a 1 mil tungsten wire mounted along the axis of the tube. Diaphragms of copper and of milar were used.

The shock waves produced by this driver were much more reproducible than those driven by explosives and were nearly constant in shock speed in contrast to the decaying speeds produced by explosives. However the incident shock Mach number produced at the end wall of the tube was only 9 to 10 for the gaseous combustion driver as compared with 11 to 15 achieved with the explosive driver.

Spectral measurements at the end wall of the tube are shown in Figures 16 and 17. The data shown in Figure 16 were taken using a driven section 25-1/2" long whereas the results of Figure 17 were obtained in a 49-5/8" long driven section. The results showed that, even in the absence

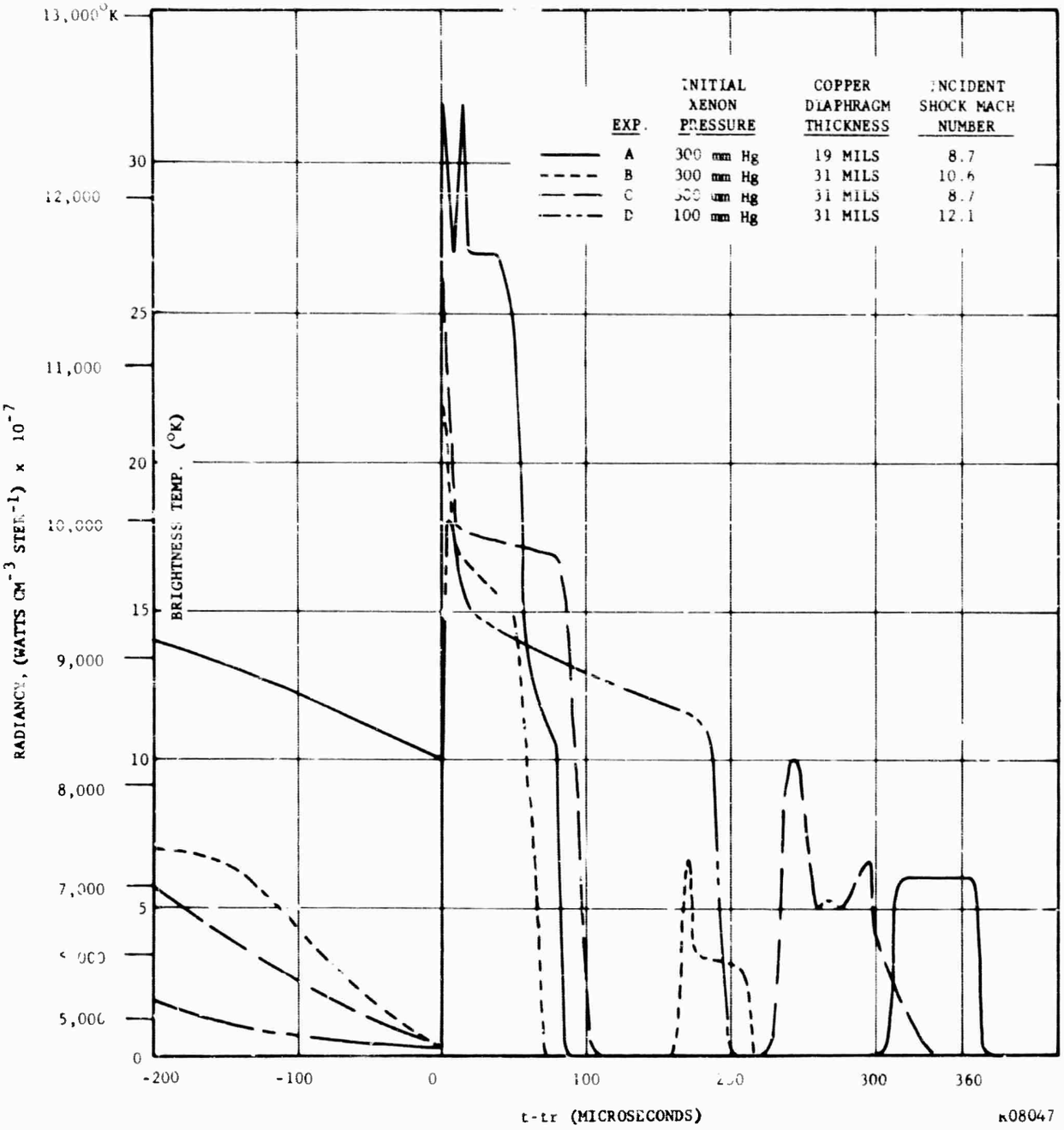

FIGURE 16. REFLECTED SHOCK RADIANCY VERSUS TIME USING THE SHORT SHOCK TUBE AND THE GASEOUS COMBUSTION DRIVER CONFIGURATION (5600A, 220A BANDWIDTH)

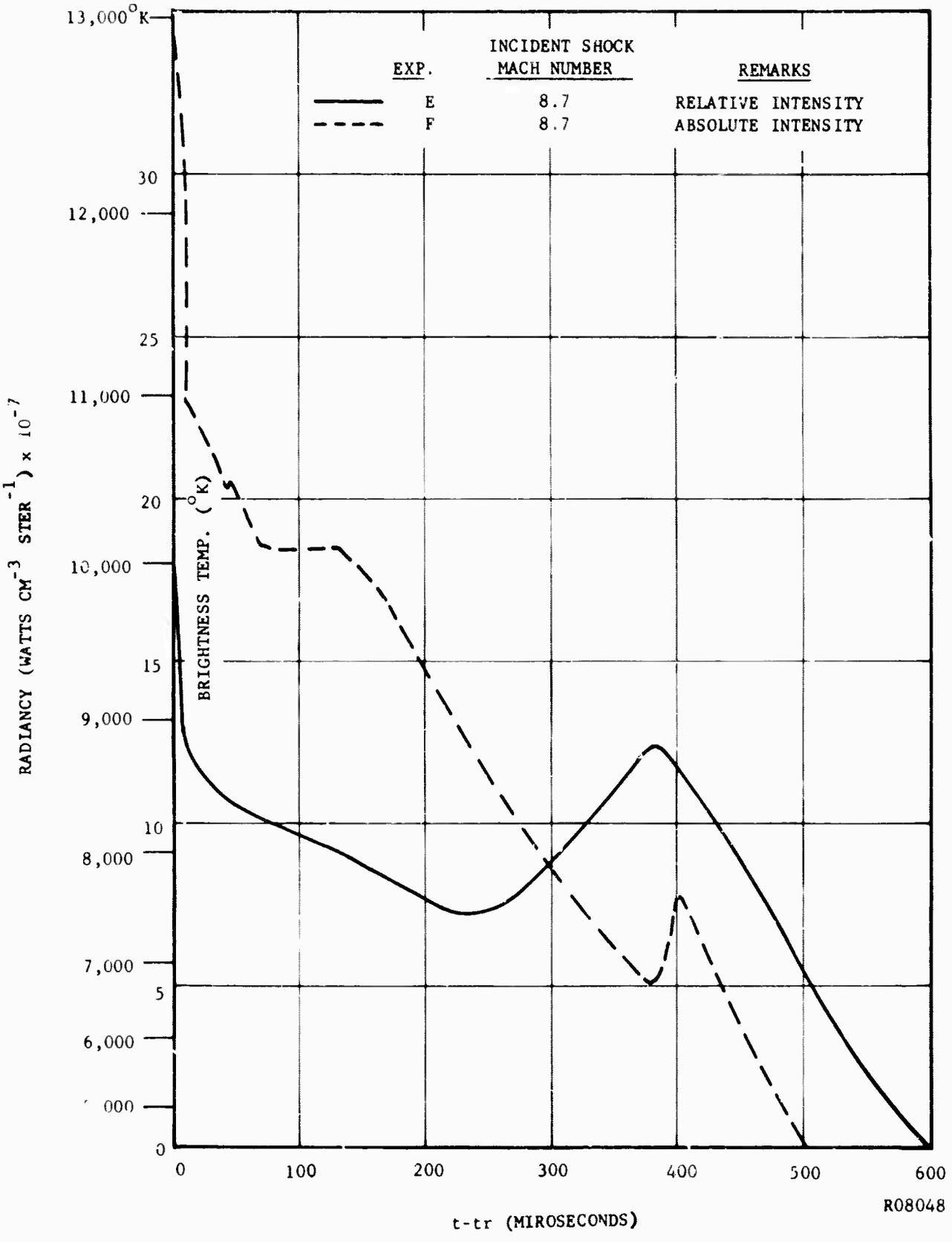

FIGURE 17. REFLECTED SHOCK RADIANCY VERSUS TIME USING THE LONG SHOCK TUBE AND THE GASEOUS COMBUSTION DRIVER CONFIGURATION (5600A, 220A BANDWIDTH, 300 mm Hg INITIAL XENON PRESSURE, 5 MIL MYLAR DIAPHRAGM

of solid particle material in the driver, a sudden radiation quenching occurs. It was found that the quenching time, i.e., the time between shock reflection and the sudden decay in radiation, depends on the diaphragm material, the initial pressure of xenon, and the tube length. All of the results are consistent with the explanation that quenching is caused by turbulent mixing of the colder gaseous driver products with the hot shock heated xenon.

In Figure 16, curve A shows a 200 μsec radiation pulse obtained in the short tube using a thin (.021") copper diaphragm. It is seen that radiation from the incident shock heated gas is very low since the shock Mach number of 8.7 produces a very low degree of ionization, resulting in low emissivity. A very rapid (< 3 μsec) rise in radiation occurs when the incident shock reflects from the end wall, bringing the xenon back to rest and approximately doubling the static enthalpy of the xenon. A brief (20 μsec) overshoot in radiation intensity occurs, due to ionization relaxation effects, and is followed by a 160 μsec plateau in radiation intensity corresponding to a brightness temperature from 10,000°K to 9000°K. The sudden quenching of radiation at 180 to 200 μsec is not typical of a radiation cooled gas and must be a result of mixing of cold material with the shock heated xenon as discussed previously. This result does show a longer duration radiation pulse than previously realized with the explosive driver, indicating that the characteristics of the driver do influence the quenching process.

However, other experiments under identical conditions showed a lack of reproducibility in the radiation pulse duration, ranging from 60 μsec to 200 μsec. Curves B and C of Figure 16 show results obtained using a heavier copper diaphragm (.032") and the same initial pressure of 300 mm Hg xenon as in Curve A. A shorter ($\sim$100 μsec) radiation pulse is seen, followed by a second pulse of about 50 μsec duration. The second radiation pulse is caused by a second shock wave generated when

the reflected primary shock interacts with the interface between shock heated xenon and combustion products. The shorter duration of the primary radiation pulse seen in curves B and C is thought to be caused by greater turbulence at the interface, due to the longer opening time of the heavier copper diaphragm. Curve D shows that at a lower xenon pressure the quenching occurs earlier, consistent with the turbulent mixing hypothesis.

Because turbulent mixing is damped by the shock tube walls and because the shocked gas volume increases linearly with tube length, the quenching should occur much later in a longer shock tube. This was verified by the results shown in Figure 17, curves E and F, which were obtained in a shock tube having a driven section 49-5/8" long as compared with the shorter tube length of 25-1/2" used for the experimental results shown in Figure 16.

Because of a lens displacement following calibration, the absolute intensity level of curve E is not known and was merely normalized to a peak brightness temperature of 10,000°K. Curve F is an absolute measurement, however, and shows a peak brightness temperature of 12,300°K. Both curves show no sudden quenching of radiation at any time, but rather the expected gradual radiation cooling curve. The total radiation pulse duration of about 500 μsec agrees well with the computed radiation cooling time. This provides further verification of the hypothesis that quenching was caused by mixing at the interface between driver and driven gases. In addition these results show that a transparent plastic window remains transparent for at least 500 μsec even when subjected to the extreme thermal and mechanical shock and subsequent convective and radiative heat flux caused by this severe environment.

The radiation pulse, curve F, has a brightness temperature greater than 10,000°K for about 170 μsec, followed by a roughly linear decay in intensity to a brightness temperature of 6000°K at 450 μsec. This performance duplicates closely that of electrically driven xenon

flash tubes suitable for stimulating laser oscillation in ruby crystals. It was achieved using only 1 gram of material containing stored chemical energy and 1.5 grams of xenon. The time integrated radiation energy output of this source is roughly equal to that of the earlier developed argon flash bomb described in Section 2.1, but uses two orders of magnitude less stored chemical energy, representing an increase in conversion efficiency from 0.1% to 10%.

2.10 LASER ACTION USING THE SHOCKED GAS CHEMICAL RADIATION SOURCE

At several points in the development of this radiation source experiments were made to test its performance in pumping laser crystals. Prior to the start of this contract a neodymium doped 1/4" x 2" calcium tungstate rod had been pumped above threshold in the coaxial geometry shown in Figure 18. This crystal had an electrically pumped threshold of 23 joules. Subsequent attempts to stimulate ruby in this configuration were not successful.

Following development of the long duration radiation source described in the previous section the laser pumping configuration shown in Figure 19 was constructed. A transition section near the end of the tube alters the circular 1" I.D. cross-section to a rectangular end wall cross-section 3/4" x 2". A 1/4" x 2" laser crystal was embedded in a thermal setting plastic in the parabolic reflecting cavity at the end wall. No laser action resulted when this configuration was used with the explosive driver to pump a ruby crystal. One attempt was made to pump ruby with this configuration at the end of the 49-5/8" long tube driven by the gaseous combustion driver, but because of instrumentation difficulties conclusive results were not obtained. The ruby crystal was recovered from the experiment completely intact.

2.11 ENERGY CONVERSION EFFICIENCY

The maximum energy conversion efficiency achieved on this program was that for the long duration pulse of Figure 17. A breakdown of the efficiency of various steps is shown in Table 2.2.

BLANK PAGE

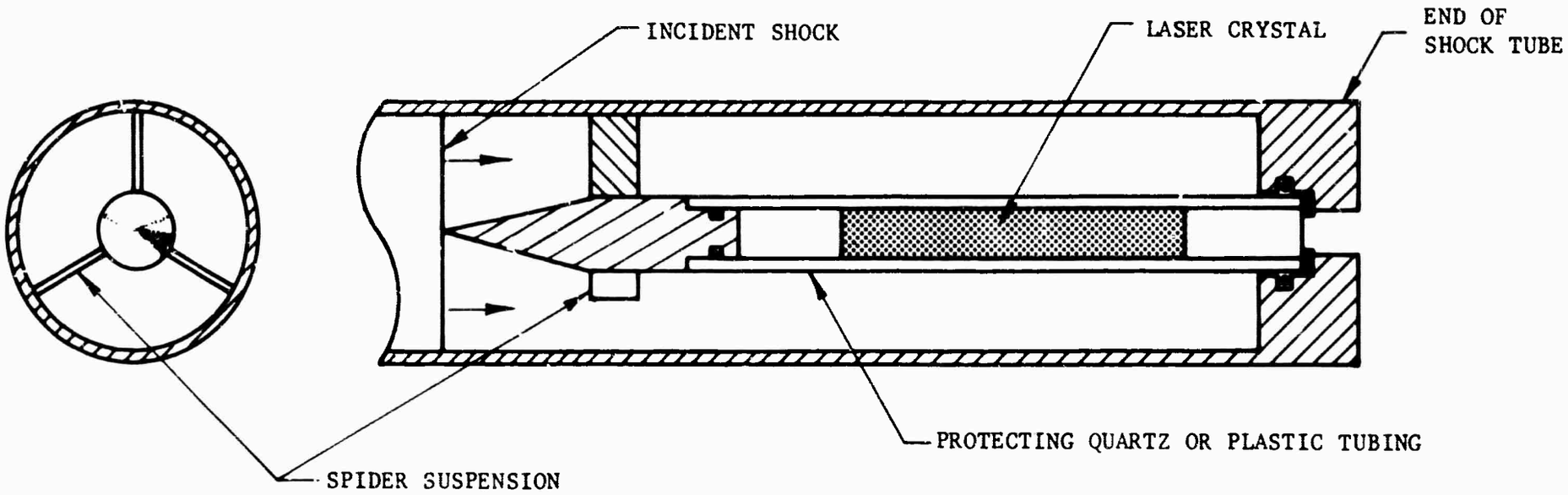

FIGURE 18. CONCENTRIC SHOCK TUBE LASER PUMPING CONFIGURATION

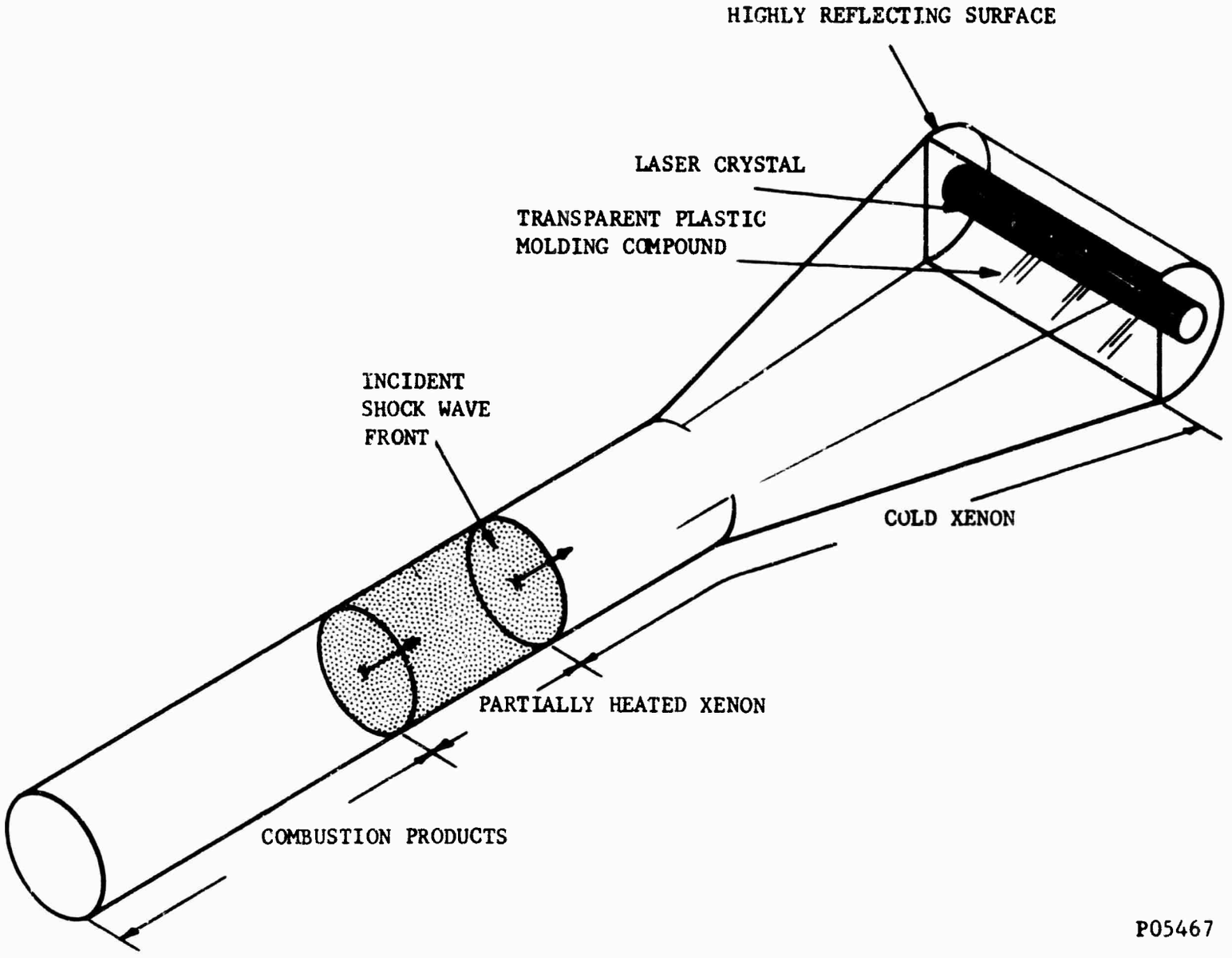

FIGURE 19. SKETCH OF THE NONDESTRUCTIVE CHEMICALLY DRIVEN REFLECTED SHOCK LASER PUMP SHOWING THE INCIDENT SHOCK WAVE TRAVELING TOWARD THE END OF THE TUBE CONTAINING THE LASER CRYSTAL

TABLE 2.2

Efficiency of Conversion of Each Energy Transformation Step Obtained Using the Gaseous Combustion Driver and the 49-5/8" Shock Tube

Form of Energy	Available Energy (joules)	Yield of Stored Chemical Energy (percent)
Gaseous combustible materials	8000	100
Shock heated gas	2100	26
Available total radiation (no mixing loss)	800	10
Actual total radiation through end wall	90	1.1
Useful spectral radiation (ruby) over 5 cm^2 surface area	9	0.1

From this table it is seen that the efficiency of converting stored chemical energy to radiation has been pushed to an acceptable value. The principal remaining causes of low energy conversion efficiency are the small spectral and geometric surface fractions utilized. These may be improved by better geometric coupling of the radiation output to the laser crystal and by making use of highly reflecting surfaces to retain radiation at wavelengths outside the pumping bands. Spectral tailoring may be utilized at somewhat lower temperatures (up to 9000°K).

2.12 PROSPECTS FOR A HIGHER POWER RADIATION SOURCE

There is a fundamental limitation in adapting this concept to the production of a much higher power source. To get appreciably higher gas temperatures it is necessary to produce initial shock Mach numbers approaching 20 in xenon, corresponding to driver speeds of 3600 m/sec in a linear shock tube, considerably higher than currently available

propellants. If explosives are used, the required speeds are achieved using shaped charges, but with the attendant mixing, and blast problems, short radiation pulse duration, and low energy conversion efficiencies. From the information gathered on this program it is concluded that the chemically driven shocked gas radiation source can be designed to operate at 15,000°K brightness temperature or less, can be non-destructive, and can yield reasonably high efficiencies. Above this temperature the efficiencies will decrease and the degree of destruction will increase.

2.13 CONCLUSIONS

The major conclusions obtained from this study of the shocked gas chemical radiation source for laser pumping are:

1. The limitations in overall energy conversion efficiency achieved previously were not fundamental, but could be overcome by (1) utilizing subatmospheric xenon driven gas, (2) using two orders of magnitude less mass of stored chemical energy, and (3) extracting radiation energy from a stationary shock heated gas.

2. Achievement of high overall energy conversion efficiency is possible at gas and radiation temperatures up to about 15,000°K. Further increase in temperature is limited because of the thermostatic effect of ionization. A fundamental limitation will preclude the simultaneous achievement of exceedingly high radiation temperatures and high overall energy conversion efficiency.

3. The development of a lightweight laser pumping system using chemical energy storage appears feasible for both neodymium doped and ruby laser crystals.

SECTION 3

PYROTECHNIC AND CHEMILUMINESCENCE STUDIES

3.1 INTRODUCTION

The studies to be described under this section have been concerned with the utilization of light arising directly from chemically reacting systems. Many chemical systems possess very high energy densities and on this basis far outstrip electrical energy storage systems presently required to pump lasers.

However, the conversion of such chemical energy to useful pump light for lasers is usually a very inefficient process. Chemical reaction energy equilibrates rapidly in the system, and the radiation output manifests itself as "thermal" radiation, that is, it is limited to the blackbody value at the system temperature. Most high temperature combustion systems, such as pyrotechnics, fall into this category. Hence, the best light sources using pyrotechnics generally implies that we seek the highest theoretical flame temperatures, coupled with near blackbody emissivities. The zirconium metal-oxygen (or solid oxidizer) system is such an example.

On the other hand, chemically reacting systems are known where non-equilibrium radiation output is observed. That is, in the course of chemical reaction, a disproportionate number of atoms or molecules may

appear in one or more higher energy states, and may radiate before they are thermally equilibrated (usually by collisional processes). Such systems may offer considerable potential for exceeding "blackbody" radiation values, and will be discussed in a subsequent section.

3.2 PYROTECHNIC STUDIES

Pyrotechnic studies have concentrated on attempting to achieve near theoretical performance from the high temperature combustion system zirconium-oxygen. While there are other metals which should yield even higher (theoretical) flame temperatures (e.g., thorium, hafnium), zirconium was selected for investigation because of its ready availability in suitable form, and, initially at least, its adequate potential as a pump source of thermal origin.

The theoretical performance of zirconium-oxygen systems is illustrated in Figures 20 and 21. Figure 20 shows the flame temperature as a function of oxygen pressure (constant throughout combustion), while Figure 21 is derived for a constant volume system at various initial oxygen pressures. In these figures, data are shown for various ratios of zirconium (solid) to oxygen. Also included are calculations for zirconium-ozone at one mixture ratio.

It is evident that increasing pressure raises the theoretical flame temperature. The most favorable mixture ratio is about stoichiometric ($Zr/c + O_2$) for both constant pressure and constant volume conditions. It is also clear that constant volume conditions are the most attractive from a practical standpoint, since relatively low initial pressures result in high final pressures which have a transitory existence. A large number of the tests to be described were carried out in sealed lucite capsules, pressurized to 10 atmospheres of oxygen initially. For a stoichiometric mixture ($Zr/c + O_2$) the theoretical flame temperature is about 6200°K, while for a mixture with twice the required oxygen ($Zr/c + 2O_2$) the predicted flame temperature is about 5650°C.

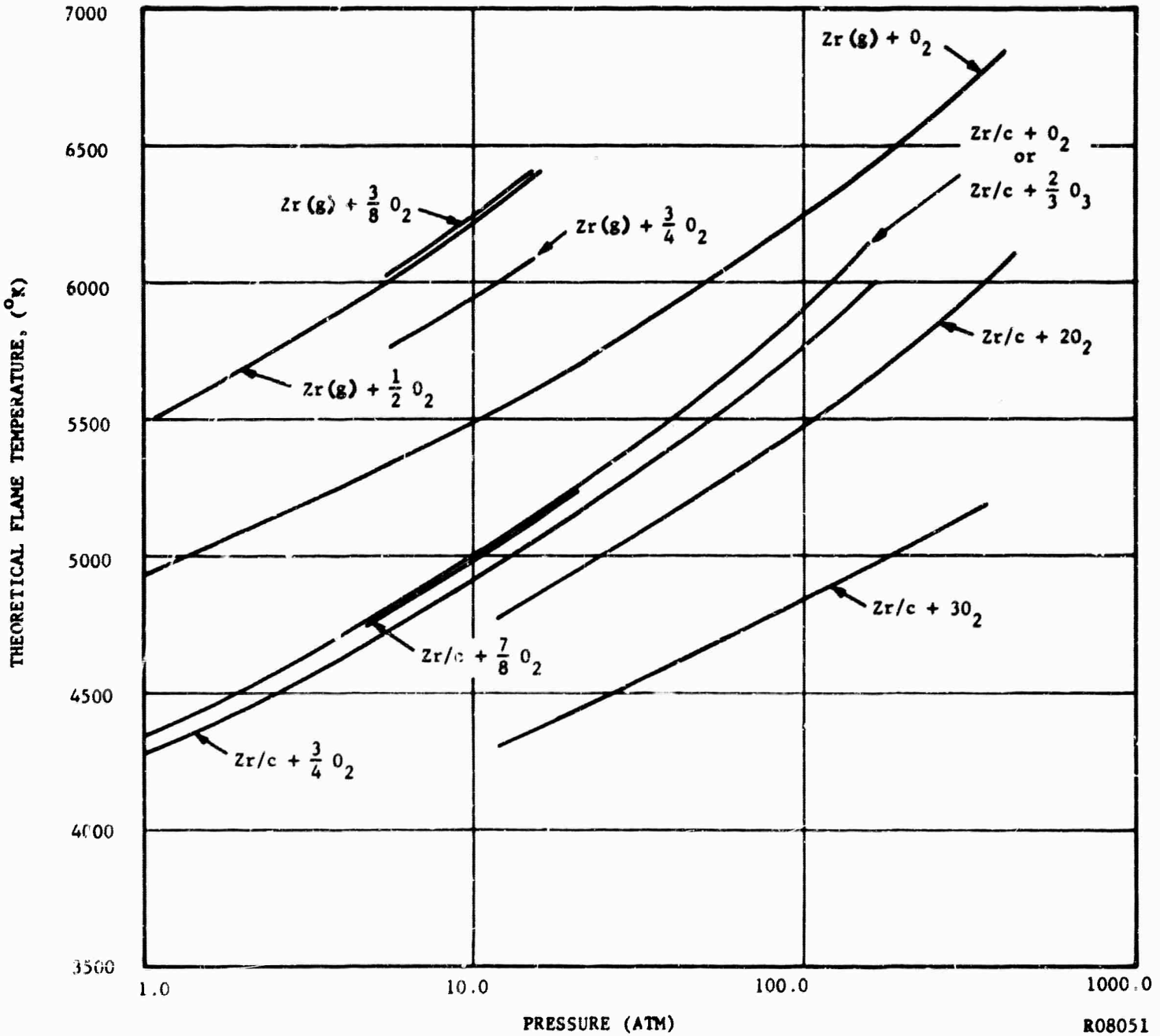

FIGURE 20. FLAME TEMPERATURES FOR Zr - O COMBUSTION AT CONSTANT PRESSURE

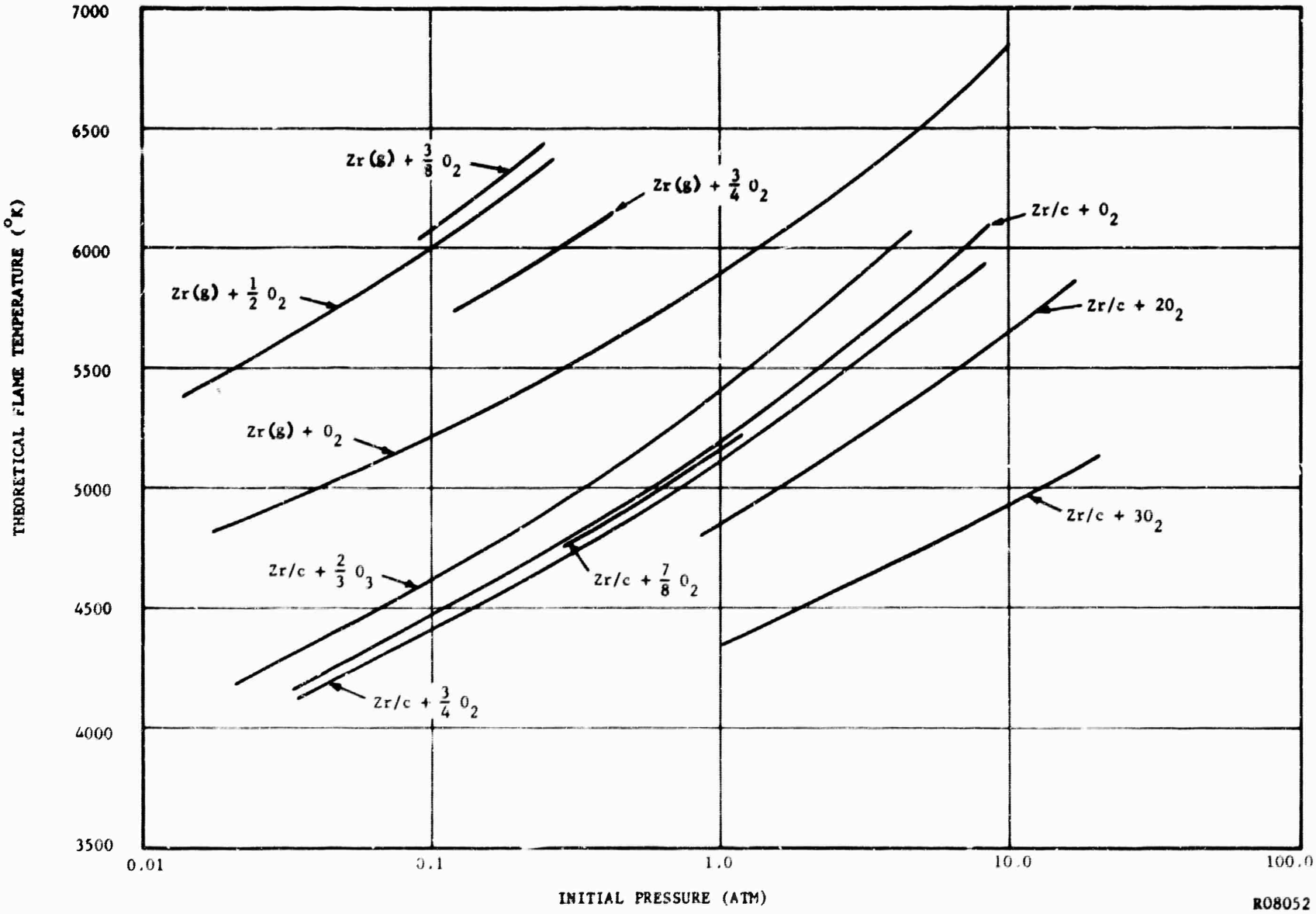

FIGURE 21. FLAME TEMPERATURES FOR Zr - O COMBUSTION AT CONSTANT VOLUME

Two modes of ignition were selected, each seeking to raise the reaction temperature through shock-heating effects. For most of the tests, 50 joules of electrical energy were discharged through the zirconium (about 4% of the chemical energy); in other tests, explosive material was set off near the burning zirconium.

Each phase of these studies is discussed below in detail.

3.2.1 Summary of Zirconium-Oxygen Studies

Tables 3.1, 3.2, 3.3, 3.4 and 3.5 summarize the data obtained on the zirconium-oxygen pyrotechnic system in the course of this program. These tables reflect the attempts made to utilize or investigate the effect of pressure increases (uniform or as a pulse), the effect of confining the reaction, the effect of salt additives, the effect of mixture ratio (stoichiometry), and optical thickness effects.

The highest brightness temperature recorded in this work for the zirconium-oxygen system is 4950°K (Table 3.5). This was achieved in a lucite cylindrical capsule, pressurized to 16 atmospheres of oxygen (oxygen/zirconium molar ratio of 2.0), and ignited with 50 joules of electrical energy. Observation of the light pulse down the axis of the tube was found to enhance slightly the optical opacity of the emitting flame as compared with transverse observation. The theoretically favored 1:1 oxygen/zirconium ratio fell considerably short of expectation (about 4500°K vs. 6200°K theoretical).

This brightness temperature of 4950°K is insufficient to pump a typical ruby laser material, although it is more than adequate to pump many neodymium-doped laser materials. The latter had been demonstrated quite some time ago in Philco Research Laboratories.

For the conditions under which the value of 4950°K was achieved, a theoretical upper limit of 5650°K is predicted (see Figure 21) for $(Zr + 2O_2)$, to which must be added a small temperature increment arising from the ignition energy supplied (approximately 50°K to 100°K).

TABLE 3.1

PERFORMANCE OF ZIRCONIUM-OXYGEN
FLASH BULBS (STANDARD M-5)

Weight of zirconium in bulb: approx. 48 milligrams
Ignition energy: approx. 2 joules (except where noted)

Oxygen Pressure, Atmos.	Peak Brightness Temp, °K	Time to Peak Radiancy, msec	Duration of Pulse, msec	Experiment Number
1-2 (est.)	4222	--	18	30
"	3900	11	--	50
"	3904	8	23	56
"	4207	14	16	62
"	4130	12	20	63
"	4043	9	18	64
"	3868	17	15	65
"	3715	17	19	66
"	4087	13	19	67
"	4180	14	17	68
"	4132	13	16	88
"	3950	11	17	94
"	4100	12	23	102
"	3918	18	22	103
"	4043(a)	5	16	69
"	3567(a)	4	9	70
1.0(b)	3556	16	23	57
2.0(b)	3702	12	15	59
10.0(b)	3935	7	11	58
10.0(b)	3935	10	20	60
73.0(b)	4226	15	16	61

(a) Ignition energy of 50 joules used, instead of 2 joules.

(b) Flashbulbs with 1/16" hole in side, placed in oxygen-pressurized optical bomb.

TABLE 3.2

EFFECT OF ZIRCONIUM-OXYGEN MIXTURE RATIO ON BRIGHTNESS TEMPERATURE

Ignition energy: 50 joules per 102 mg of zirconium
Sealed lucite capsules, 1/8" wall thickness (except as noted) glass lined

Oxygen/ Zirconium Mole Ratio	Weight of Zirconium, mg	Initial Oxygen Pressure, Atmos.	Peak Brightness Temp, ^{o}K	Time to Peak Temp, msec	Duration of Pulse, msec	Experiment Number
1.0	102	5	4046	0.52	2	89(a)
1.0	102	5	4286	0.32	1.37	90
1.0	102	5	4371	0.26	0.56	91
1.0	204	10	4388	0.34	1.39	93(b)
2.0	102	10	4535	0.40	0.76	46
2.0	102	10	4104	0.21	--	47
2.0	102	10	4246	0.80	--	48
2.0	102	10	4519	0.23	--	95
2.0	102	10	4193	0.62	1.75	96

(a) Heavy-wall lucite capsule employed, 1/2" thick; also glass end plates.

(b) 100 joules ignition energy used.

TABLE 3.3

EFFECT OF DOPING ZIRCONIUM METAL
WITH VARIOUS SALTS

Salts deposited on zirconium by evaporation from solution
Ignition energy: 50 joules
Weight of zirconium used: 102 milligrams
Sealed lucite capsules, 1/8" wall thickness (except as noted), glass-lined
Initial Oxygen Pressure: 10 atmos (except as noted)

Doping Salt	Weight of Salt, mg	Oxygen/ Zirconium Mole Ratio	Peak Brightness Temp, °K	Time to Peak Temp, msec	Duration of Pulse, msec	Experiment Number
Barium Nitrate	5	2.0	4651	0.20	0.22	78
"	6	2.0	4685	0.24	0.54	79
"	35	2.0	4621	0.16	0.20	74
"	34	2.0	4542	0.12	0.24	75
"	34	2.0	4542	0.20	0.28	77
Cesium Nitrate	54	2.0	4652	0.32	--	76
"	5	4.0	4919	--	0.52	29(a)
Sodium Chloride	5	4.0	4722	--	0.20	28(a)
Cesium Nitrate	8	2.0	4118	0.60	1.10	72(b)
"	6	2.0	4400	0.15	0.60	73(b)
Barium Nitrate	5	1.0	4430	0.22	1.20	82(b)
Barium Chloride (Dihydrate)	6	2.0	4193	0.10	0.70	71(b)

(a) Data taken 12/10/63 when calibration was in question, hence temperatures are considered erroneous.

(b) Heavy-wall lucite capsule employed, 1/2" thick; also glass end plates.

TABLE 3.4

EFFECT OF EXPLOSIVE PULSE
ON ZIRCONIUM-OXYGEN BRIGHTNESS TEMPERATURES

Explosive used: Central core of 110 mg of lead styphnate, encased in thin teflon tube
Initial oxygen pressure: 10 atmos
Ignition energy: 50 joules per 102 mg of zirconium (except as noted); energy was split between zirconium wool and explosive ignition wire
Sealed lucite capsules, 1/8" wall thickness, glass lined

Oxygen/ Zirconium Mole Ratio	Weight of Zirconium, mg	Peak Brightness Temp, ^{o}K	Time to Peak Temp, msec	Duration of Pulse, msec	Experiment Number
4.0	102	2720	0.72	0.32	38(a)
2.0	102	4790	0.12	0.30	84
2.0	102	4503	0.36	--	85
2.0	102	4651	0.20	--	86
2.0	102	4828	0.30	--	87
1.0	204	4068	0.14	0.22	97
1.0	204	4739	0.22	--	98(b)
1.0	204	4590	0.12	0.20	105(b)(c)

(a) Lead styphnate ignited with 3 mil nichrome wire, 2 joules electrical energy; zirconium was not ignited prior to setting off explosive.

(b) Zirconium doped with approx. 11 milligrams Barium Nitrate salt.

(c) Flat mirror placed behind capsule to double the optical thickness.

TABLE 3.5

EFFECT OF COMBUSTION OPTICAL THICKNESS
ON OBSERVED BRIGHTNESS TEMPERATURES

Sealed lucite capsules, 1/8" wall thickness (except as noted), glass lined
Brightness temperatures taken from end view of capsule
Ignition Energy: 50 joules per 102 milligrams of zirconium
Initial Oxygen Pressure: 10 atmos (except as noted)

Oxygen/ Zirconium Mole Ratio	Weight of Zirconium mg	Peak Brightness Temp, °K	Time to Peak Temp, msec	Duration of Pulse, msec	Experiment Number
2.0	102	4950	0.010	0.66	99
2.0	102	4270	0.16	0.42	100(a)
1.0	204	4509	0.040	0.20	101
1.2	102	4625	0.060	0.55	104(b)
1.2	102	4559	0.040	0.80	106(b)

(a) Capacitor supplying ignition energy failed to discharge completely.

(b) Heavy-wall lucite capsule employed, 1/2" thick, glass and plates. Six atmospheres of oxygen pressurization supplied initially instead of ten.

Considering the various loss mechanisms which can degrade the performance of the system, the 800°K "deficit" is not an excessive one. Needless to say, there is considerable variability in the data under apparently similar conditions, a circumstance which appears to be entirely due to non-uniform combustion. This, in turn, is related to the variable way in which the ignition energy discharges through the heterogeneous mass of zirconium wool. Instrumental or operator error in the temperature measurements is no more than $\pm$ 100°K.

The great variability in the brightness temperature data render it difficult to assess accurately the effect of particular parameters. Nevertheless it is highly instructive to examine the data in this way, since they would appear to be applicable to other metal-oxidizer systems.

(a) Effect of Pressure on Brightness Temperature

Table 3.1 is illustrative of the effect of pressure on measured brightness temperature. The data are for standard M-5 flashbulbs, which contain about 48 mg of zirconium wool in a mildly pressurized atmosphere of oxygen. The first sixteen pieces of data were obtained on the as-received, sealed bulbs, and it is seen that the measured brightness temperatures range from about 3500°K to 4200°K. A small hole was drilled in the glass envelope (allowing a constant pressure environment) and the bulbs so treated were ignited in an optical bomb, at various oxygen pressures. The temperatures rose with increasing pressure, ranging from about 3500°K at 1 atmosphere to about 4200°K at 73 atmospheres.

It is interesting to note that the sealed bulbs give similar performance to that shown by the 10 atmosphere constant pressure experiment, and Figure 21 predicts that the final pressure of such sealed bulbs will be about 10 atmospheres, theoretically.

It is abundantly clear from Figures 20 and 21, and the experimental data obtained in the "constant volume" lucite capsules, that

pressurization is essential to realizing higher temperatures. It also tends to reduce combustion time and hence reduce heat losses which degrade the peak temperature achieved. Throughout the tabulated data there will appear results obtained in extra-heavy walled lucite tubes, whose purpose was to better contain the pressures developed. No appreciable benefit was noted, possibly due to the extra transmission losses so introduced.

(b) Effect of Zirconium-Oxygen Mixture Ratio

Table 3.2 shows data illustrating the effect of altering the oxygen-zirconium ratio. A molar ratio of unity is, theoretically, the one giving very nearly the highest flame temperature with solid zirconium. However, these and other data (e.g., Table 3.4) appear to show no advantage for the 1:1 ratio over the 2:1 ratio. In fact, there appears to be a tendency in the other direction, possibly due to oxygen-starvation of the burning metal (whose oxygen is supplied by diffusion from the gas phase). For an initial oxygen pressure of 10 atmospheres (constant volume) a peak theoretical temperature of about 6200°K is predicted for a 1:1 ratio. The best values achieved were 1500°K or more below this.

(c) Effect of Doping Zirconium Metal with Salts

A number of experiments were carried out to determine the effect of "doping" the zirconium metal with various salts. Three possible benefits were anticipated: (1) the use of solid oxidizers could provide a high final pressure without incurring prohibitive high initial pressures, (2) optical opacity, and hence system emissivity would be increased, and (3) chemiluminescent effects might be achieved, resulting in higher brightness temperatures in the desired spectral regions.

Table 3.3 summarizes the results of such tests. It appears that the presence of such salts enhanced the observed brightness temperatures (cf. Table 3.2). In all probability, the major effect is due to an increased number of radiators per cm^3 (greater optical opacity). The small amounts of oxidizers employed would not be expected to result

in significantly higher final pressures, and, in fact, their presence conceivably would theoretically degrade the peak flame temperature achieved. A similar enhancement may have occurred in Experiments 98 and 105 (see Table 3.4; also compare with Table 3.2).

(d) Effect of Chemical Explosive on Combustion

The majority of experiments described were conducted with 50 joules of electrical energy deposited in the zirconium wool. This was intended both as an ignition source and to provide shock heating effects. A number of experiments were carried out in which a central core of thermally sensitive explosive (lead styphnate) was detonated while surrounded by the zirconium wool. In this way, an approach would be made to an all-chemical system utilizing the principle described. These results are tabulated in Table 3.4. There appears to be definite benefit from the introduction of an explosive pulse during the combustion of zirconium-oxygen (e.g., compare Table 3.2). Clearly there is variability in the data, and the utilization of extra energy in this way has not yet been optimized. It seems highly probable that the maximum benefits of such shock heating are realized when the pressure pulse passes through the already-burning zirconium, rather than when the latter is in the incipient ignition state. Time did not permit a thorough check on whether this requirement was met in the various experiments listed in Table 3.5.

(e) Effect of Optical Thickness on Observed Temperatures

Previously (Section 3.2) we noted that our observed brightness temperature will, in general, be lower than the particle temperature composing the radiating combustion cloud. To have the system radiate like a blackbody corresponding to the system temperature requires a sufficient optical depth, which is given approximately by the mean free path, λ, for a photon in the system: $\lambda \cong 1/Nd^2$, with N radiating particles of diameter d per cm^3. Unfortunately, it is not possible to establish d a priori. In this work, we have assumed that spherical particles of

zirconium oxide are formed during combustion, of diameter equal to or less than the original zirconium wire diameter, of about 25 microns. If 0.102 grams zirconium are used, and the system volume is 7 cm^3, the value of λ is about 1 cm. This is very close to the inner diameter of the capsules used for these experiments, and indicates the definite possibility of low optical emissivity resulting from small optical depth.

Experiments shown in Table 3.5 were undertaken to investigate this aspect. Normally, the lucite reaction tubes were viewed from the side; for most of these tests, the tubes were viewed end-on, which should provide about 7 to 8 times the normal optical thickness.

The results appear to confirm the crude calculations, and show a small improvement in observed brightness temperature. In fact, the highest temperature observed in the pyrotechnic program was recorded in this series, namely 4950°K (Experiment #99). The data may be compared to those listed in Table 3.2, where observations were taken from the side aspect entirely.

3.2.2 Summary of Explosive Injection Studies

A limited number of specialized experiments were carried out in an attempt to explosively inject metal fuels into an oxidizing atmosphere. It was hoped that sufficient metal vaporization would occur, coupled with pressure effects to obtain substantial brightness temperatures.

The apparatus employed for this purpose is illustrated in Figure 22. It consists of a lower compartment which houses an explosive charge, above which is placed the metal to be injected. Above this is a glass tube containing the oxidizing gas (oxygen in these experiments), which is separated from the lower compartment by a light diaphragm. The explosive is set off, and the metal is partially vaporized and moves with high velocity into the oxidizing gas where it reacts. As shown in Figures 20 and 21, the reaction between gaseous zirconium and oxygen yield very high theoretical temperatures, particularly in constant volume systems.

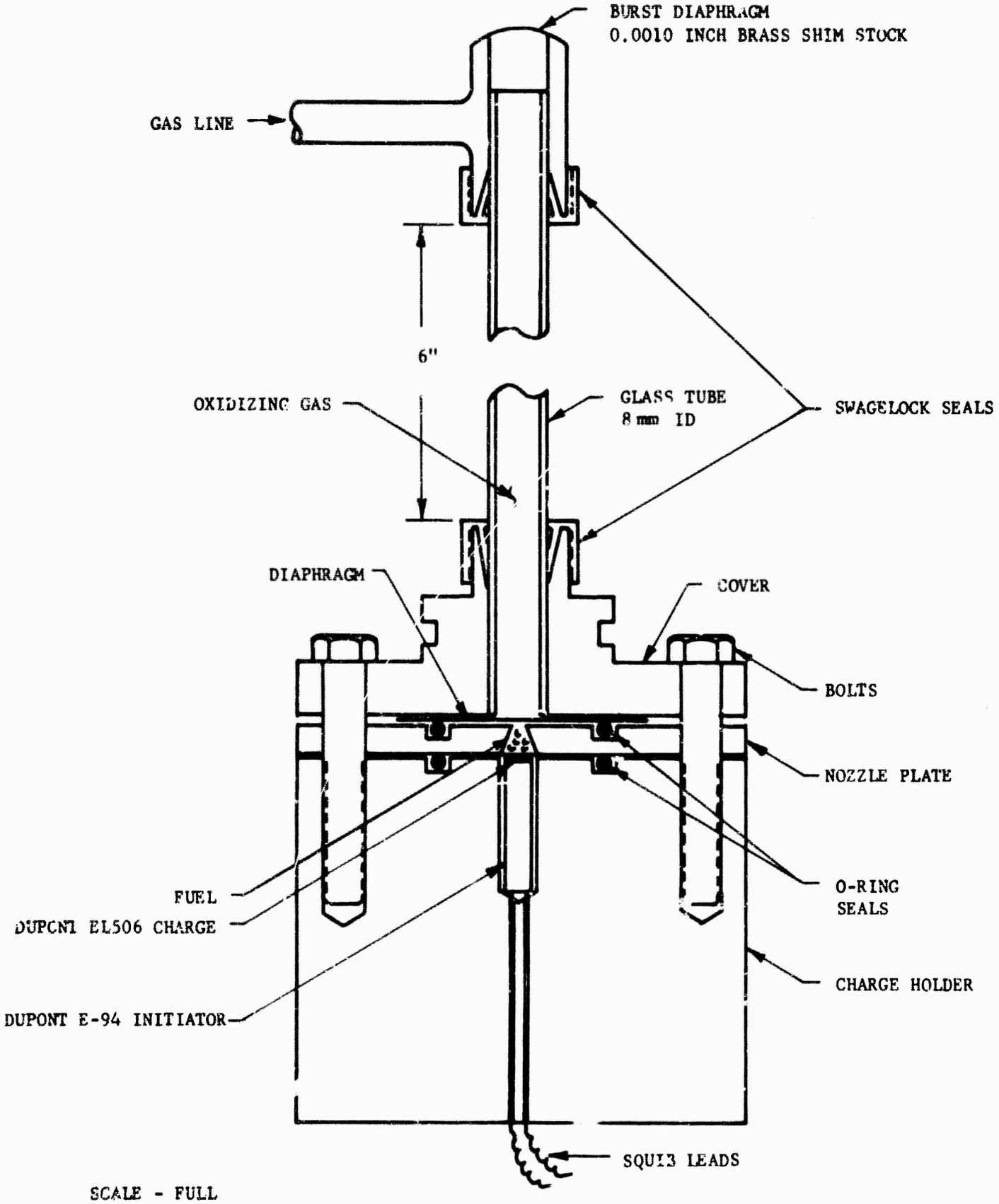

FIGURE 22. APPARATUS FOR INVESTIGATING EXPLOSIVE INJECTION OF METALS

It was soon found that the amount of explosive which had to be used to effect any significant vaporization (or impart significant kinetic energy) was prohibitive to this apparatus. None of the actual tests conducted produced enough light to expose the spectrograph film used to check the character of light output. No absolute temperatures were recorded because of the very low light intensities obtained. By eye it was observed that boron metal gave yellow to blue or blue-white flames, and barium gave a green flame (all in oxygen).

3.3 CHEMILUMINESCENCE STUDIES

Chemiluminescence (or "anomalous" excitation during chemical reaction) refers to those phenomena where chemical reaction energy, originally converted to atomic or molecular internal energy, appears directly as radiation. The radiating species are present in non-equilibrium concentrations, and hence thermal equilibrium has not yet been established in the system by usual collisional processes. Among the best known examples of chemiluminescence may be listed: (a) the luminol or "cold light" system, (b) the reaction between sodium vapor and chlorine gas at low pressures,[7] and (c) a wide variety of observations in hydrocarbon and hydrogen-oxygen flames with or without traces of metals.[8] In the last case, some probable sources of "anomalous" excitation are:

$$H + H + \text{Metal} \longrightarrow H_2 + \text{Metal}^*$$

or

$$H + OH + \text{Metal} \longrightarrow H_2O + \text{Metal}^* \qquad (1)$$

where "Metal*" denotes an electronically excited metal atom. The energy for excitation is, of course, derived from the energy of reaction.

Most recently, J. C. Polanyi and his associates have done extensive work in infrared chemiluminescence, both experimental and theoretical in character. One of the reaction systems which was investigated in detail was:

$$H + Cl_2 \longrightarrow HCl^{v} + Cl \qquad (2)$$

This chemical reaction is mildly exothermic, and at sufficiently low pressures it is found that practically all the reaction energy turns up as vibrational energy in the product molecule HCl, which is thus denoted as HCl^{v} (in its ground electronic state). Polanyi has shown that this is a common occurrence in chemically reacting systems, where the energy of reaction is liberated as the products of reaction separate. The vibrationally-excited HCl in (2) is deactivated relatively slowly by collision and, as a result, is able to radiate from these non-equilibrium, high energy levels. Spectroscopic analysis shows a markedly non-Boltzmann vibrational energy distribution, being characterized by "temperatures" ranging from 8000°K to 2930°K.[9]

As a result of work of this kind, Polanyi proposed that certain chemically reacting systems might lend themselves to laser action directly, in view of the large population inversion of vibrational energy states which they showed.[10]

From the standpoint of achieving useful pump light for materials like ruby, it is necessary to consider systems undergoing electronic transitions. Generally speaking, where atoms are the radiating species, the line widths are too narrow to deposit much useful energy in the ruby pumping band. A broadband radiator, that is, molecular in origin, is required.

It should be noted that in order for a chemiluminescent source to be of ultimate practical significance, it must provide radiant power in excess of the thermal equilibrium or blackbody value for the system. Clearly it is possible to have a population inversion of excited states giving chemiluminescence, but having so few radiators per unit volume that little radiant power results. For example, iron exhibits chemiluminescent effects in hydrogen-oxygen flames. This can be inferred by spectroscopic

analysis which reveals that in the reaction zone of the flame, the distribution of energy states in the blue end of the spectrum corresponds to a much higher "temperature" than the actual flame temperature. At very low iron concentrations, the system would be so thin optically that the intensity from this source is arbitrarily low. In order to realize benefits corresponding to the non-equilibrium "temperature", the concentration of radiators must be increased. In some cases, the absolute spectral intensity of iron has been observed to exceed that which would result from the theoretical flame temperature.[8] Usually, those processes which must be used to increase radiant power also result in an enhancement of deactivation mechanisms. Thus, increasing the concentration of radiators, often increases collisional deactivation of excited species, which promotes the approach to thermal equilibrium of the system.

One of the experiments in this program where chemiluminescence was observed was described in the Third Quarterly Technical Report. Strontium nitrate powder was fed into the oxygen line of a hydrogen-oxygen torch. The gaseous flow rates were adjusted to give the maximum light intensity. Spectroscopic observations of the 6060Å strontium line were taken and the brightness temperature was found to be as high as 3300°K. Theoretical flame temperature calculations were made, and it was found that any finite amount of strontium nitrate in the optimum hydrogen-oxygen mixture would reduce the theoretical flame temperature below that for hydrogen-oxygen alone, namely about 3070°K (see Figure 23). Thus, a non-equilibrium temperature advantage of at least several hundred degrees was realized through chemiluminescence. The observed effect was concentrated in the flame reaction zone.

Another experiment of this kind using barium peroxide did not show such effects. The highest brightness temperature recorded (~5137Å) was about 2750°K which might easily correspond to theoretical prediction based on thermodynamic equilibrium (as illustrated in Figure 24).

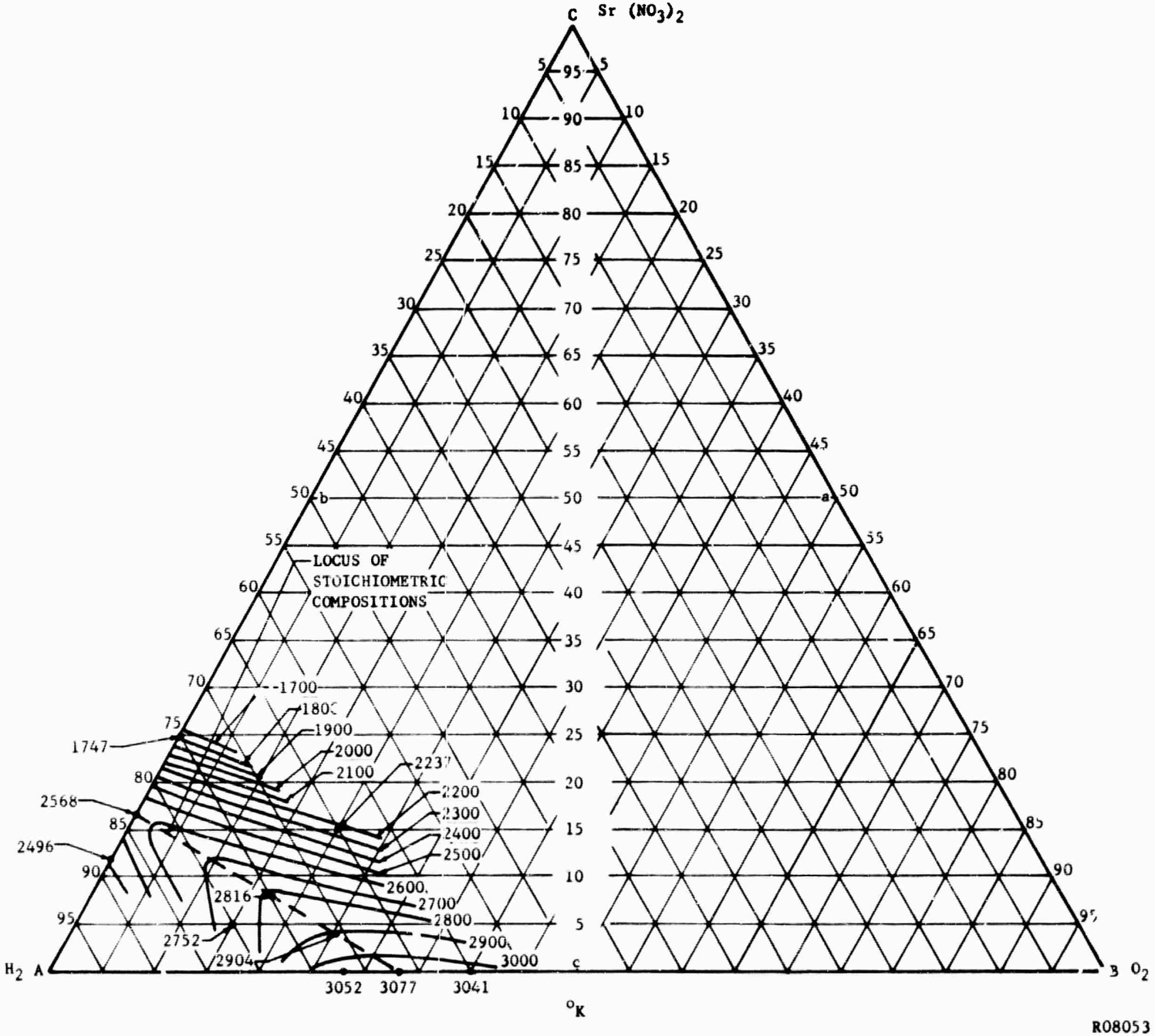

FIGURE 23. THEORETICAL FLAME TEMPERATURE CONTOURS FOR MIXTURES OF HYDROGEN, OXYGEN AND STRONTIUM NITRATE (PRESSURE = 1 ATMOS; MIXTURES IN MOLE %)

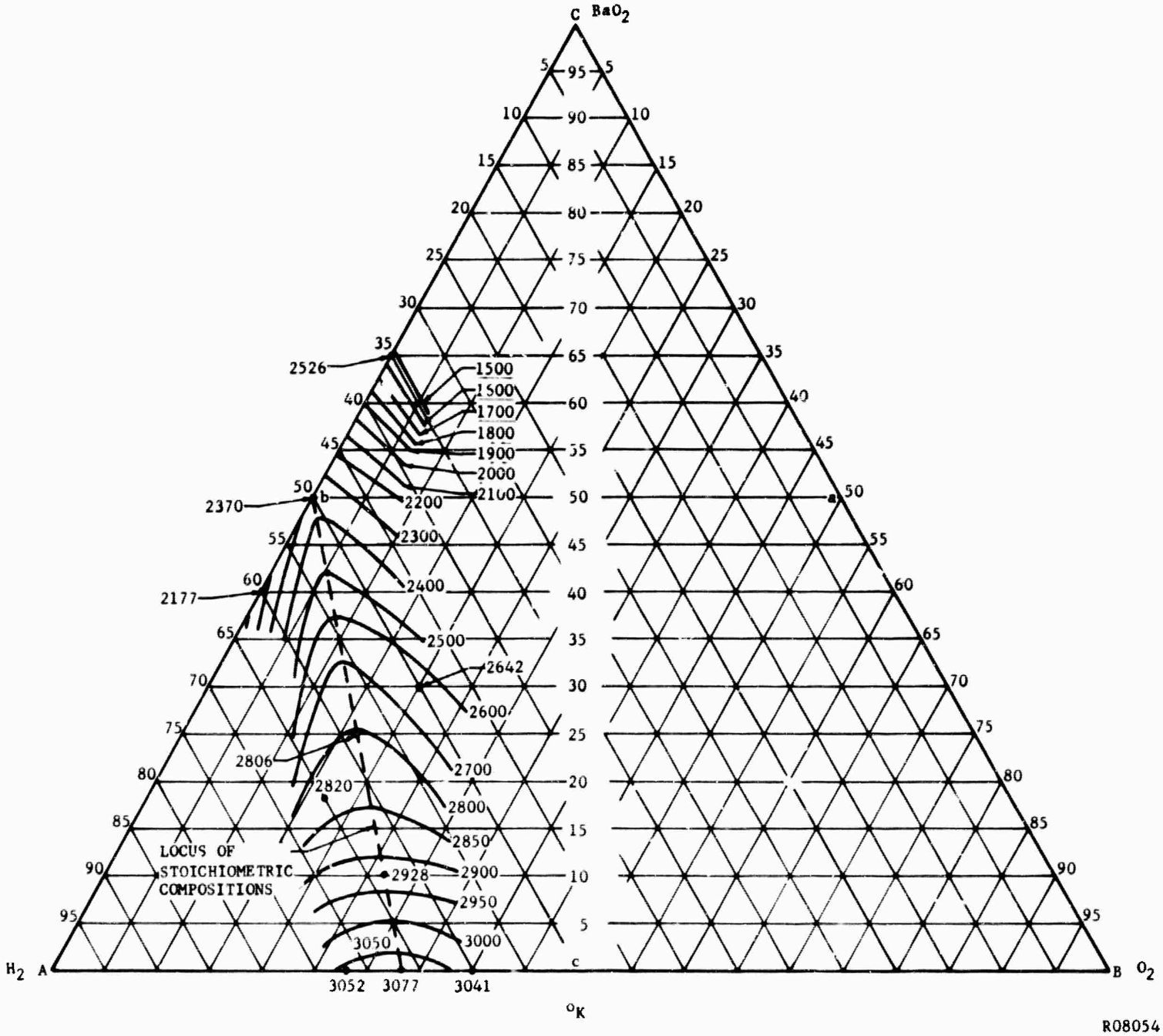

FIGURE 24. THEORETICAL FLAME TEMPERATURE CONTOURS FOR MIXTURES OF HYDROGEN, OXYGEN AND BARIUM PEROXIDE (PRESSURE = 1 ATMOS; MIXTURES IN MOLE %)

Finally, as described in Section 3.2.2, an attempt was made to observe possible chemiluminescent effects during the explosive injection experiment. This failed, as noted, due to the very low intensities obtained.

It should be possible to seek chemiluminescent pump sources based on the following considerations. A number of elementary chemical reactions can be selected which have a high heat of reaction associated with them. If we wish to radiate 5000Å quanta, the exothermicity must be about 2.5 e.v. (or 58 kcal/mole). One might then consider reactions of the following kind, in which the resulting stable molecular species is in an electronically excited state:

$$A + BC \longrightarrow AB^* + C(\text{exothermic}) \qquad (3)$$

where AB* denotes the electronically excited molecule AB. This may suffer de-excitation through collision before it is able to radiate:

$$AB^* + M(\text{any third body}) \longrightarrow AB + M(\text{deactivation}) \qquad (4)$$

$$AB^* \longrightarrow AB + h\nu\ (\text{radiation}) \qquad (5)$$

It is not clear under what conditions we may expect the reaction energy in (3) to finally manifest itself as electronic excitation in the product molecule. An example of a suitably energetic reaction would be:

$$Mg(g) + F_2 \longrightarrow MgF(g) + F \qquad (6)$$

Here the energy of reaction is about 93 kcal/mole. Other possible reactions are:

$$Ca(g) + F_2 \longrightarrow CaF + F\ (108\ \text{kcal/mole}) \qquad (7)$$

$$La(g) + O_2 \longrightarrow LaO + O\ (66\ \text{kcal/mole}) \qquad (8)$$

$$B(s) + F_2 \longrightarrow BF + F\ (58\ \text{kcal/mole}) \qquad (9)$$

It will be noted that reactions (6), (7) and (8) require that the metal fuel be introduced as a vapor in order to realize an overall exothermicity of the amount shown. This, of course, requires the expenditure of energy and reduces the overall efficiency. However, even if the potential efficiency were reduced by a factor of two in this way, chemical pumping would still be very attractive relative to current electrical sources used with solid state laser materials.

REFERENCES

1. W. Lochte-Holtgreven, Reports on Progress in Physics, 21, 312 (1958), M. A. Cook, "The Science of High Explosives," Reinhold, New York (1958).

2. L. I. Sedov, "Similarity and Dimensional Methods in Mechanics," Academic Press, New York, 1959.

3. H. E. Petschek, et.al., J. Appl. Phys. 26, 83 (1955).

4. H. N. Olsen, Phys. Rev. 124, 1703 (1961).

5. J. Pomerantz, J. Quant. Spect. Rad. Trans. 1, 185 (1961).

6. H. W. Liepmann and A. Roshko, "Elements of Gas Dynamics," Wiley, New York, 1957.

7. Polanyi, "Atomic Reactions" (Williams and Norgate, London, 1932).

8. Gaydon and Wolfhard, Proc. Roy. Soc. (London) A 205, 118 (1951).

9. Charters and Polanyi, Disc. of Far. Soc. Number 33, 1962.

10. Polanyi, J. Chem. Phys. 34, 347 (1961).